Quaternary Research 81 (2014) 21–34

Contents lists available at ScienceDirect

Quaternary Research

journal homepage: www.elsevier.com/locate/yqres

Recognizing cryptic environmental changes by using paleoecology and taphonomy of Pleistocene bivalve assemblages in the Oga Peninsula, northern Japan

Tomoki Chiba [a,*], Masaaki Shirai [b], Shin'ichi Sato [c]

[a] Institute of Geology and Paleontology, Graduate School of Science, Tohoku University, Aoba 6-3, Aramaki, Aoba-ku, Sendai 980-8578, Japan
[b] Department of Geography, Tokyo Metropolitan University, 1-1 Minami-Osawa, Hachioji 192-0397, Japan
[c] The Tohoku University Museum, Aoba 6-3, Aramaki, Aoba-ku, Sendai 980-8578, Japan

ARTICLE INFO

Article history:
Received 13 April 2013
Available online 14 November 2013

Keywords:
Bivalve
Mollusk
Paleoecology
Taphonomy
Shell concentration
Sedimentary facies
Bay
Shelf
Crustal movement
Multivariate analysis

ABSTRACT

Multivariate analyses applied to Pleistocene bivalve assemblages from the Oga Peninsula (northern Japan) discriminate three distinct assemblages. The assemblages and their taphonomy were used to recognize environmental settings and changes. The *Astarte–Cyclocardia–Glycymeris* assemblage indicates shelf environment (below the storm wave base) where gravels and shells are transported from shallower settings. Supply of the exotic coarse sediment probably enabled epifaunal bivalves to inhabit the sea floor. The *Glycymeris* assemblage is characterized by dominance of *G. yessoensis* and represents current-swept shoreface environment (above the storm wave base). The *Moerella* assemblage is characterized by bivalves inhabiting bay to open-marine conditions and diverse deposit-feeders, indicating a moderately land-locked environment, such as an open bay or a bay mouth. Fine-grained substrata rich in organic matters in the bay were probably suitable for the deposit-feeders. Ordination also shows the assemblages along two environmental gradients, a bathymetrical one and the other related to open-marine and bay conditions. The environmental changes are explained mainly by glacio-eustatic sea-level changes and alternation of coastal geomorphology caused by local crustal movements. This study also suggests that fossil assemblages can be a powerful tool to reconstruct environments and depositional dynamics even in intensely bioturbated sedimentary facies.

Introduction

Paleoecology and taphonomy have been frequently used for reconstructing environmental and sedimentological conditions. Since the appearance of sequence stratigraphy, analyses in fossil assemblages have been high-resolution (systems tract and finer scales), and recurrences of shell beds and fossil assemblages have been explained mainly by sea-level fluctuations and related changes in environment and sedimentation (Kidwell, 1991; Brett, 1995, 1998; Kondo et al., 1998). Recently, many studies have demonstrated that multivariate analyses can empirically recognize interpretable fossil assemblages and extract environmental gradients in Europe (e.g., Dominici, 2001; Scarponi and Kowalewski, 2004; Zuschin et al., 2007), America (e.g., Holland et al., 2001; Daley, 2002; Leonard-Pingel et al., 2012) and New Zealand (e.g., Abbott and Carter, 1997; Hendy and Kamp, 2004, 2007). In addition, recent taphonomic studies on modern marine environments have suggested that taphonomic features (e.g., abrasion, encrustation, fragmentation of shells) as well as fossil assemblages can be used to characterize ancient environmental settings and changes (e.g., Tomašových and Zuschin, 2009; Powell et al., 2011; Brett et al., 2013).

For Quaternary fossil assemblages in particular, knowledge of the environmental distributions of extant relatives can be used to reconstruct environment (e.g., absolute water depth and salinity) through taxonomic uniformitarianism (e.g., Scarponi and Kowalewski, 2004; Dominici et al., 2008; Carboni et al., 2010). In addition, environmental changes inferred from fossil assemblages refine sedimentary dynamics and sequence stratigraphy (e.g., Abbott, 1997; Abbott and Carter, 1997). Furthermore, environmental conditions also provide important information for paleobiology and paleoecology (e.g., evolution and biotic interaction) since changes in shell morphology and predator–prey interaction (e.g., location of predatory drillhole on prey skeleton) may be induced by environmental changes (e.g., Daley, 2002; Daley et al., 2007). However, environmental reconstructions on the basis of macrofossil assemblages and their taphonomy are relatively rare in Japan partly because of scarcity of a continuous outcrop and limited variation in the macrofossil assemblages.

The Oga Peninsula is a type locality for Quaternary sediments of Japan Sea side of northern Japan (Kano et al., 2011). In particular, the Oga Peninsula bears continuous shallow-marine successions that have been uplifted above present sea-level as a result of crustal movements (Shirai and Tada, 2002). In addition, the successions are rich in well-preserved

* Corresponding author.
E-mail addresses: tc-fossil@nifty.com (T. Chiba), mshirai@tmu.ac.jp (M. Shirai), kurosato@m.tohoku.ac.jp (S. Sato).

0033-5894/$ – see front matter © 2013 University of Washington. Published by Elsevier Inc. All rights reserved.
http://dx.doi.org/10.1016/j.yqres.2013.10.015

mollusk fossils (Ogasawara et al., 1986), making these successions suitable for the study of mollusk assemblages and environmental reconstructions. Many studies have described the mollusk fossils for each formation (e.g., Takayasu, 1962; Huzioka et al., 1970; Watanabe, 2004). However, no high-resolution quantitative study of the mollusk fossils has been performed, despite the potential importance of the mollusk fossils as an archive for environmental changes. Although, Shuto et al. (1977) have reported mollusk fossil assemblages from the Anden Coast (1 in Fig. 1C), they have not reconstructed environments using the mollusk assemblages. In addition, relationships between the mollusk assemblages and sedimentary facies remain unexplored. This is because of the scarcity of knowledge of recent mollusks (e.g., geographic and bathymetric distributions) and lack of sequence stratigraphic framework. After the Shuto et al.'s (1977) pioneer work, knowledge of recent mollusks has been accumulated and updated around the Japanese Islands (Okutani, 2000; Japanese Association of Benthology, 2012), and sequence stratigraphy has been established (Shirai and Tada, 1997, 2000). It is, therefore, timely to re-analyze the mollusk fossil assemblages.

Here, we quantitatively examined the Pleistocene mollusk fossil assemblages in the Oga Peninsula. We hypothesize that the mollusk assemblages indicate fluctuations in water depth, as sedimentary facies of the shallow-marine succession reflect glacio-eustatic sea-level changes (Shirai and Tada, 1997, 2000). In addition, available literature on sedimentary successions from tectonically active regions shows that basin tectonics as well as glacio-eustatic sea-level changes affect water depth and sedimentation (e.g., Ito et al., 1999; Zecchin, 2005). Because the Oga Peninsula is characterized by active crustal movements during the Quaternary period (Shirai and Tada, 2002), we expect the crustal movements cause environmental changes. If so, the environmental changes caused by crustal movements can be recognized by looking at composition of the mollusk assemblages, as they can be sensitive to the environmental changes (e.g., Dominici, 2001). The aims of this study are (1) to describe bivalve assemblages using multivariate techniques, (2) to reconstruct environments, (3) to explore relationship between the bivalve assemblages and sedimentary facies and (4) to refine interpretation of depositional dynamics in the Oga Peninsula.

Geology and stratigraphy

Cenozoic sedimentary and volcanic rocks are well exposed in the Oga Peninsula, Akita Prefecture, northern Japan (Kano et al., 2011). The late Cenozoic strata in the Oga Peninsula dip eastward and become younger to the east, from Miocene to Holocene (Fig. 1C). The Quaternary sediments are divided into the Kitaura, Wakimoto, Shibikawa, Katanishi, Iriai, Hakoi and Hashimoto formations, in ascending order (Kano et al., 2011). The depositional environments of these formations change from continental slope (the Kitaura Formation) through shelf and nearshore (the Wakimoto, Shibikawa and Katanishi formations) to non-marine (the Iriai, Hakoi and Hashimoto formations) (Kitazato, 1975; Shirai and Tada, 2000; Shiraishi, 2000).

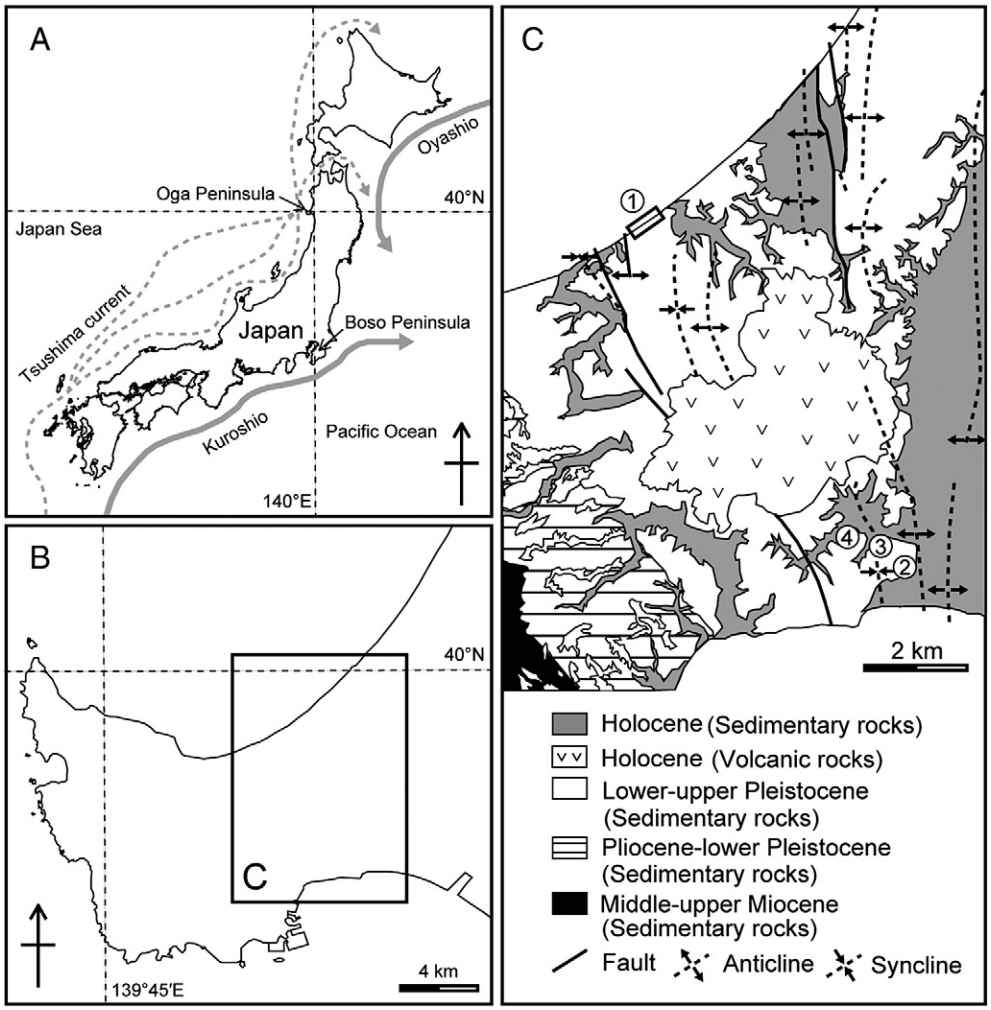

Figure 1. A–B. Map showing location of the Oga Peninsula, Akita Prefecture, northern Japan. Generalized recent current systems around the Japanese Islands are shown (after Kitamura et al., 2000). C. Geologic map of eastern part of the Oga Peninsula. Locations of outcrops (1: Anden Coast, 2: Wakimoto-1, 3: Wakimoto-2, 4: Tayasawa) are shown. The base map from Kano et al. (2011).

https://doi.org/10.1016/j.yqres.2013.10.015 Published online by Cambridge University Press

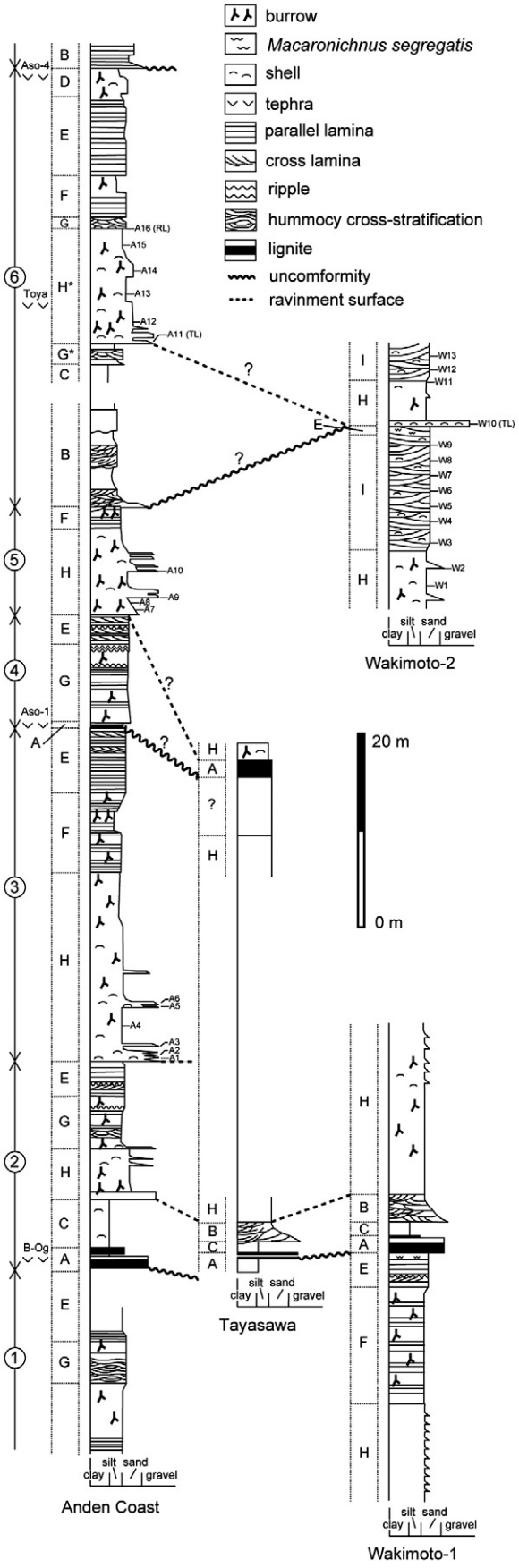

Many studies on the middle–upper Pleistocene Shibikawa and Katanishi formations have been performed in the Anden Coast and Wakimoto area (1–3 in Fig. 1C), including tephrochronology (Shiraishi et al., 1992; Shirai et al., 1997), stratigraphy (Okada, 1979; Shirai and Tada, 1997, 2000) and investigation on crustal movement (Shirai and Tada, 2002). In particular, Shirai and Tada (2000) have described sedimentary facies from a continuous section along the Anden Coast and estimated depositional environments and water depths of each sedimentary facies. They have compared the depositional depth curve from the Anden Coast with the $\delta^{18}O$ curve (Imbrie et al., 1984) and confirmed that the sedimentary cycles mainly reflect fifth- and sixth-order glacio-eustatic sea-level changes between approximately 80 and 450 ka. The present study followed Shirai and Tada's (2000) sequence stratigraphic interpretation, with an exception of position of sequence boundary dividing cycles 5 and 6 (Fig. 2). The sequence boundary should be better placed between facies F and B of cycle 5 in Shirai and Tada (2000), which is corrected in Shiraishi et al. (2008).

Sedimentary facies

Nine sedimentary facies (facies A–H; Table 1) have been recognized from the Shibikawa and Katanishi formations in the Anden Coast by Shirai and Tada (2000). We applied this interpretation to Wakimoto and Tayasawa areas (2–4 in Fig. 1C), and facies H* and I are designated based on the present study (Table 1). We used the present sub-bottom sedimentary features observed in coastal systems around the Oga Peninsula (Saito, 1988, 1989) to estimate absolute water depth of each sedimentary facies as in Shirai and Tada (2000). Here, we briefly explain characteristics of four sedimentary facies focused in the present study (see Shirai and Tada, 2000, for full descriptions). The rest of sedimentary facies are described in Supplementary Text.

Facies G consists of brownish-gray, well-sorted fine-grained sandstone associated with hummocky cross-stratification, with occasional intercalations of brown, poorly-sorted, bioturbated siltstones. The facies G was deposited at the lower-shoreface to inner-shelf (water depth =20–60 m, under the fair-weather wave base and above the storm wave base).

Facies H consists of brownish-gray, poorly sorted, massive, fine-grained, silty sandstone with intercalations of granule- to cobble-size gravels and shells. The layers show poor sorting, normal grading and sharp bases. Facies H was deposited at the inner- to middle-shelf (water depth = 60–100 m, below the storm wave base).

Facies I, which is independently designated based on the present study from Wakimoto area, consists of gray well-sorted medium- to coarse-grained sandstone associated with trough cross-stratification (Fig. 3E). Currents inferred from the trough cross-stratification show various directions. The sandy sediment without silt represents deposition above the fair-weather wave base (water depth < 20 m; Saito, 1988, 1989). This inference is supported by abundant occurrence of articulated shells of *Glycymeris yessoensis* (Fig. 3E) which inhabits recent subtidal zone (5–30 m) around the Japanese Islands (Matsukuma, 1986; Okutani, 2000). The variously oriented trough cross-stratifications interpreted as being formed by longshore and/or rip currents in shoreface environment (e.g., Reimnitz et al., 1976; Greenwood and Davidson-Arnott, 1979) agree well with our estimation. Therefore, the depositional environment of facies I is interpreted as the current-swept shoreface (water depth = 5–20 m).

Facies H* is also independently designated based on the present study and will be explained later, with taking bivalve assemblages into consideration (see Discussion).

Figure 2. Columnar sections along the Anden Coast, Tayasawa, Wakimoto-1 and Wakimoto-2. Capital letters A through H and circled numbers represent facies code and sedimentary cycle number, respectively (Table 1). A boundary between facies H and facies H* at the Anden Coast is gradual (see Discussion). Sampling horizons (A1–16 and W1–13) are shown. TL: transgressive lag deposit, RL: regressive lag deposit. Columnar section of Anden Coast modified from Shirai and Tada (2000). Dated marker tephras are B-Og (448 ka), Aso-1 (255 ka), Toya (112 ka) and Aso-4 (88 ka) (Shirai et al., 1997).

https://doi.org/10.1016/j.yqres.2013.10.015 Published online by Cambridge University Press

Table 1
Classification of sedimentary facies (modified from Shirai and Tada, 2000). Facies code, lithologic features and depositional environments are summarized. Facies H* and I are independently designated by the present study. Bold faces represent additional descriptions from Wakimoto area based on the present study.

Facies code	Major lithology	Sedimentary structure	Other lithologic features	Depositional environment and depth
A	Lignite	Horizonal stratification, slump	Wood fragments and stumps	Coastal swamp (−20–0 m)
B	Siltstone intercalating medium sandstone–pebble	Slump (siltstone), epsilon-cross and trough stratification (sandstone)	Rich in carbonaceous matter (siltstone)	Flood plain (−20–0 m)
C	Claystone	Massive or parallel laminae	Rich in carbonaceous matter, *Corbicula*[a], *Trapa*[a]	Salt marsh (−1–1 m)
D	Fine silty sandstone	Massive	Drift pumice, *Corbicula*[a], intense bioturbation	Lagoon-bay (0–10 m)
E	Very fine-fine sandstone	Parallel laminae, planar and trough cross laminae, and ripple	Concentrations of magnetite or pumice, ***Macaronichnus segregatis*, Rootlet**	Backshore, foreshore and upper shoreface (0–10 m)
F	Fine sandstone and siltstone	Subhorizonal laminae (sandstone)	Bioturbated (siltstone)	Middle-lower shoreface (10–20 m)
G	Fine sandstone intercalating siltstone	Hummocky cross stratification	Bioturbated (siltstone)	Lower shoreface-inner shelf (20–60 m)
G*	Fine silty sandstone and siltstone	Hummocky cross stratification (sandstone)	Poor sorting (sandstone), rich in carbonaceous matter	Coastal lagoon-enclosed bay (<60 m)
H	Fine silty sandstone	Massive	Intense bioturbation, sand-gravel and shell beds	Inner-middle shelf (60–100 m)
H*	Fine silty sandstone	Massive	Intense bioturbation, rich in carbonaceous matter, *Rosselia socialis*	Open bay-bay mouth (10–50 m)
I	**Medium-coarse sandstone**	**Trough cross stratification**	**Good sorting, *Glycymeris yessoensis***	**Upper-lower shoreface (5–20 m)**

[a] Kato and Watanabe (1976).

Sedimentary cycles

Shirai and Tada (2000) have reported six sedimentary cycles (cycle 1–6) in the Anden Coast, associated with two lignite layers (Fig. 2). The lignite layers were used as key-beds to correlate sections of Wakimoto and Tayasawa areas to that of the Anden Coast. The lower lignite layer is intercalated in thick Oga pumice tuff and thus can be discriminated from the upper lignite layer.

Sedimentary facies succession shows that Wakimoto-1 section (2 in Fig. 1C) consists of two sedimentary cycles (Fig. 2). The lower lignite layer is intercalated in Wakimoto-1 section, and thus the two sedimentary cycles are correlated with cycles 1 and 2 (Fig. 2). Sedimentary facies succession shows that Tayasawa section (4 in Fig. 1C) consists of three sedimentary cycles (Fig. 2). The lower and upper lignite layers are intercalated in Tayasawa section. The three sedimentary cycles in Tayasawa section are probably correlated with cycles 2, 3 and 5 (Fig. 2). Cycle 4 is the only sedimentary cycle which does not accompany facies H (Fig. 2), and cycles 4 and 5 are correlated with marine oxygen isotope substages 7.4–8.2 and 7.2–7.4, respectively (Shirai and Tada, 2000). All sedimentary cycles in Tayasawa section include facies H, and thus we interpret that cycle 4 was eroded by cycle 5, or cycles 4 and 5 were amalgamated in Tayasawa section. Sedimentary facies succession shows Wakimoto-2 section (3 in Fig. 1C) consists of two sedimentary cycles, although no lignite layer is intercalated in Wakimoto-2 section (Fig. 2). When outcrop was well exposed, the upper lignite layer occurred below the lower cycle of Wakimoto-2 section (Okada, 1979; Watanabe personal communication, 2012). In addition, Okada (1979) found Toya tephra (a light purple tuff bed in Okada, 1979) from adjacent section (Wakimoto to Iinomori in Okada, 1979) of Wakimoto-2 section, and the horizon bearing Toya tephra was correlated with the upper cycle of Wakimoto-2 section. In Anden Coast section, Toya tephra occurs in cycle 6 (Fig. 2). Therefore, the lower and upper cycles of Wakimoto-2 section are tentatively correlated with cycles 5 and 6, respectively (Fig. 2).

Materials and methods

Sampling and processing

Bioclastic fabrics for each sampling horizon were described in the field. Descriptive terms for the bioclastic fabrics (i.e., orientation, articulation, packing and sorting) employed herein were based on Kidwell et al. (1986) and Kidwell and Holland (1991).

We excavated 29 bulk samples (25 × 25 cm, 20 cm depth) parallel to bedding plane from main shell beds of Anden Coast section (15 samples from facies H and one sample from facies G) and Wakimoto-2 section (four samples from facies H and nine samples from facies I) (Fig. 2). The bulk samples were collected from three of nine sedimentary facies (facies G, H and I) because the other facies did not contain shells with reasonable sample sizes for statistical analyses. We did not take a bulk sample from cycle 2 because most shells were fragmented and could not be identified with confidence. Well-preserved or large-bodied macrofossils were manually picked around each horizon, but not included in the following statistical analyses.

The bulk samples were wet-sieved using 2-mm mesh in the laboratory. We picked up all mollusk shells if umbo/apex was preserved, and only unbroken bivalve shells were included. The bivalve shells were major component of macrofossils in the samples. Furthermore, genus-level identification was possible for most of the bivalve taxa. As in Scarponi and Kowalewski (2004), we counted a valve as 0.5 individual (specimen) because a bivalve individual consists of two valves.

Analytical method

We recorded 24,345 bivalve specimens (41 families, 84 genera and 104 species) from 29 bulk samples. Of these, we lumped together several species (e.g., *Astarte alaskensis*, *Astarte borealis* and *Astarte hakodatensis*) under a genus (e.g., *Astarte* spp.) owing to difficulty of species-level identification. For this reason, we obtained a data matrix consists of 98 taxa (Supplementary Tables 1 and 2). Selected macrofossil specimens are deposited at the Tohoku University Museum (IGPS coll. cat. nos. 111208–111369).

All rare taxa (total abundance < 30 specimens) were excluded prior to multivariate analyses because occurrences of the rare taxa depend on chance only. Our final data matrix included 44 taxa 23,845 bivalve specimens. The sample sizes ranged from 53 to 2699 (average = 822; Supplementary Tables 1 and 2). The final data matrix was converted to relative abundance within each sample and then square-root transformed (i.e., Hellinger transformation in Legendre and Gallagher, 2001) to compensate for difference in sample sizes and to down-weight dominant taxa.

Q-mode and R-mode cluster analyses were performed to recognize bivalve assemblages. Clustering applied here was agglomerative nesting with Ward's method, which adds samples to existing clusters based on minimizing the total sum of squares. Ward's method tends to produce discrete clusters that are different one another (Legendre and Legendre, 2012). For Q-mode and R-mode clusterings, Bray–Curtis dissimilarity and 1-Spearman's rho were used, respectively. These coefficients are often used in numerical ecology (Borcard et al., 2011). The results of cluster analyses were shown by dendrograms together with a matrix of relative abundance.

https://doi.org/10.1016/j.yqres.2013.10.015 Published online by Cambridge University Press

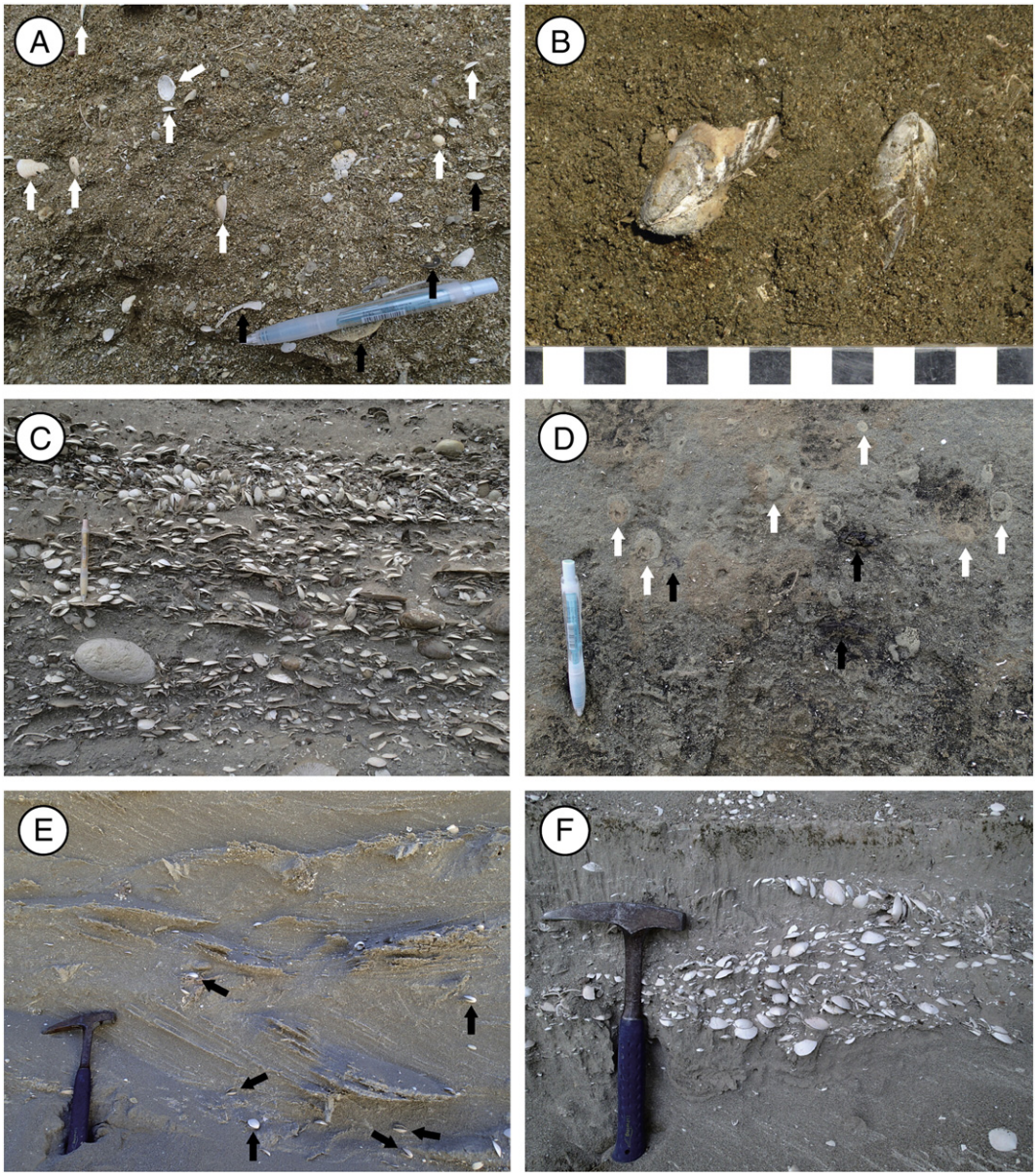

Figure 3. Field photographs of sedimentary facies and shell concentrations. A. Loosely/densely packed sedimentological accumulation (Type 1 shell concentration, A9 horizon). White and black arrows represent disarticulated shells of *Glycymeris yessoensis* and *Mizuhopecten yessoensis*, respectively. B. *Modiolus modiolus* preserved in life orientation (horizontal exposure, W1 horizon). These specimens are deposited at the Tohoku University Museum (IGPS coll. cat. no. 111208). C. Densely packed sedimentological accumulation (Type 2 shell concentration, W10 horizon). D. Dispersed biogenic accumulation (Type 3 shell concentration, A13 horizon). *Rosselia socialis* (white arrows) and wood fragments (black arrows) occurs in massive fine-grained silty sandstone (sedimentary facies H*; Table 1). E. Dispersed or loosely packed biogenic/sedimentological accumulation (Type 4 shell concentration, W5 horizon). Articulated shells of *G. yessoensis* (black arrows) are common. Trough cross-stratification occurs in medium- to fine-grained sandstone (sedimentary facies I; Table 1). F. Loosely/densely packed sedimentological accumulation (Type 5 shell concentration, W3 horizon). Pen = 15 cm (A, C and D).

Because cluster analyses have tendency to break gradients into discrete assemblages, an ordination was performed. This analysis was used to understand how bivalve assemblages intergraded along biotic gradients and to recognize the main underlying environmental factors. Non-metric multidimentional scaling (NMDS) is a robust ordination method which does not distort the second axis due to a detrending procedure (Minchin, 1987; Bush and Brame, 2010). Detrended correspondence analysis (DCA) has been frequently applied to paleoecology (e.g., Holland et al., 2001; Scarponi and Kowalewski, 2004), but the scores along the second axis can be meaningless because of the detrending procedure (Bush and Brame, 2010; Borcard et al., 2011). Therefore, NMDS ordination using Bray–Curtis dissimilarity was selected here. As in cluster analyses, Hellinger transformation was applied prior to NMDS. To evaluate differences in composition of bivalve assemblages among sedimentary facies and types of shell concentration, we performed permutational multivariate analysis of variance (PERMANOVA, Anderson, 2001) using Bray–Curtis dissimilarity with 5000 permutations. PERMANOVA is similar to analysis of similarity (ANOSIM, Clarke, 1993), but it is based on raw rather than on rank-order distances, and it is less sensitive to among-group differences in variances (Anderson, 2001). All statistical analyses were performed using vegan package in R statistical environment (R Development Core Team, 2009; Oksanen et al., 2012).

Ecology of recent bivalves

A majority of bivalve taxa (ca. 99%) collected from the bulk samples are living around the Japanese Islands. We, therefore, used ecology of recent bivalves to infer environment. Bathymetric distributions of the bivalve taxa were based on Japanese literatures (Habe, 1961; Habe and Ito, 1965; Oyama, 1973; Okutani, 2000). After Okutani (2000), we

https://doi.org/10.1016/j.yqres.2013.10.015 Published online by Cambridge University Press

categorized the bivalve taxa into "warm-water taxa" "cold-water taxa" and "cosmopolitan taxa" which respectively inhabit the area south of 35°N latitude, north of 35°N latitude and both areas of the Japanese Islands in general (Fig. 1A). Because the warm Kuroshio Current, which increases water temperature and supplies larvae of marine organisms, leaves the Japanese Islands at the Boso Peninsula at 35°N latitude (Fig. 1A), a sharp boundary of the marine biogeography can be recognized in this area (e.g., Horikoshi, 1962). The definition has been widely used both in ecology (e.g., Kurihara et al., 2011) and paleontology (e.g., Kanazawa, 1990; Kitamura et al., 1994).

The bivalve taxa were assigned to functional groups on the basis of their relationships to the substrata (infaunal or epifaunal), diet (suspension-feeder, deposit-feeder, chemosymbiotic or carnivore) and attachment (byssally attached or cemented). Information on the functional groups was based on worldwide and Japanese literatures (Wada et al., 1996; Huber, 2010; Japanese Association of Benthology, 2012). The analysis in functional groups enables to reconstruct environment, in a mechanistically supported way, including substrata consistency (e.g., Kondo, 1998; Leonard-Pingel et al., 2012) and food availability (e.g., Rhoads et al., 1972; Todd et al., 2002).

Results

Mode of shell concentration

Five types of shell concentration are discriminated in terms of relationship between shells and matrix, geometry, shell-size distribution, shell orientations and preservation state of shells (e.g., disarticulation/articulation, abrasion, bioerosion and encrustation) based on field observation at the Anden Coast, Wakimoto and Tayasawa areas (Type 1–5 shell concentrations; Table 2).

Type 1 shell concentration is characterized by shells of varying sizes loosely/densely packed in poorly sorted fine-grained silty sandstone (Fig. 3A). The shell concentration shows bed-like geometry and normal grading. In the shell concentration, thick-shelled taxa (e.g., *G. yessoensis* and *Mizuhopecten yessoensis*) are abundant (Fig. 3A). A majority of shells are disarticulated and randomly oriented (Fig. 3A). Preservation state of the shells varies from pristine to poor (i.e., physically abraded, bioeroded and encrusted). The poorly preserved shells are common in comparison with Type 3–5 shell concentrations (see below). Some shells of *M. yessoensis* and *Swiftopecten swifti* are discolored (black shells in Fig 3A). *Modiolus modiolus* shells are occasionally found in life orientation (Fig. 3B). Some bivalves (e.g., *Cyclocardia nipponensis*, *A. borealis*, *Limopsis crenata*, *Nuculana pernula* and *G. yessoensis*) and brachiopods are found, with their valves articulated, but not in life orientations.

Type 2 shell concentration is densely packed in basal parts of facies G/H in association with pebble- to cobble-sized gravels (Fig. 3C). The shell concentration shows bed-like geometry (Fig. 3C). In the concentration, thick-shelled taxa (e.g., *G. yessoensis* and *M. yessoensis*) are abundant. The shells >30 mm in maximum dimension are abundant compared to the other shell concentrations, suggesting size sorting of shells. In general, shells are disarticulated, with concordant to oblique and convex-upward orientations (Fig. 3C). Shells heavily altered by physical abrasion, bioerosion and encrustation are common.

Type 3 shell concentration is characterized by shells of varying sizes dispersed in fine-grained silty sandstone (Fig. 3D). In the concentration, thin-shelled taxa (e.g., *Moerella jedoensis* and *Nitidotellina hokkaidoensis*) are abundant. Pristine shells are common in the concentration. For some articulated shells (e.g., *G. yessoensis*, *Panopea japonica*, *Lucinoma annulatum*, *Solecurtus divaricatus*, *Macoma tokyoensis* and *Felaniella usta*), ligament and periostracum are preserved (Fig. 4). In addition, deep-borrowers (*P. japonica* and *L. annulatum*) are found in life orientation.

Type 4 shell concentration is characterized by shells of varying sizes dispersed or loosely packed in medium- to coarse-grained sandstone (Fig. 3E). In the concentration, *G. yessoensis* shells are abundant. The articulated shells are common and show concordant to oblique orientations (Fig. 3E). *Glycymeris yessoensis* shells occur in variable states of preservation, including articulated pristine shells, and slightly or moderately abraded disarticulated shells, but not in life orientation. *Panopea japonica* is found in life orientation.

Type 5 shell concentration is characterized by shells of varying sizes loosely/densely packed in medium- to coarse-grained sandstone (Fig. 3F). The shell concentration shows lens-like geometry (Fig. 3F). In the concentration, *G. yessoensis* shells are abundant, and the shells are generally found in concordant to oblique and convex-upward orientations. A majority of the shells are disarticulated, and some shells show imbrications (Fig. 3F). Preservation state of *G. yessoensis* varies from pristine to abraded shells as in Type 4 shell concentration.

Cluster analyses

The R-mode cluster analysis shows three groups of commonly co-occurring taxa (cluster 1–3; Fig. 5). The Q-mode cluster analysis also yields three groups (cluster A–C; Fig. 5) corresponding to assemblages. Interestingly, samples from facies H are divided into two clusters (clusters A and B; Fig. 5). The assemblages are named after characteristic taxa, selected because of their high relative abundance within a given assemblage (Fig. 6).

The *Astarte–Cyclocardia–Glycymeris* assemblage (13 samples in cluster A; Fig. 5) is characterized by dominance of *G. yessoensis*, *Cyclocardia* spp. and *Astarte* spp. (mean relative abundance ± SE = 19.8 ± 3.6, 14.5 ± 3.6 and 14.2 ± 1.9, respectively; Fig. 6A). The samples of the assemblage occur in facies H of cycles 3 and 5 (Figs. 2 and 5). Characteristic

Table 2
Classification of shell concentrations. Descriptive terminology based on Kidwell et al. (1986) and Kidwell and Holland (1991).

Type	Biofabric			Geometry	Internal structure	Assemblage type	Concentration type	Corresponding bivalve assemblage, sedimentary facies and environment[a]
	Packing	Size sorting	Orientation					
Type 1	Loose/dense	Unsorted	Mostly random, rarely life orientation	Bed	Simple	Mostly allochthonous, rarely autochthonous	Mostly sedimentologic, rarely biogenic	Cluster A, Facies H (Inner-middle shelf)
Type 2	Dense	Sorted	Mostly concordant and convex-upward	Bed	Simple	Allochthonous	Sedimentologic	None
Type 3	Disperse	Unsorted	Mostly random/rarely life orientation	Irregular	None	Parautochthonous/ autochthonous	Mostly biogenic	Cluster B, Facies H* (Open bay-bay mouth)
Type 4	Disperse/loose	Unsorted	Oblique/concordant	Irregular	None	Parautochthonous	Biogenic/sedimentologic	Cluster C, Facies I (Upper-lower shoreface)
Type 5	Loose/dense	Unsorted	Oblique/concordant, convex-upward, imbricaion	Lens	Simple	Allochthonous	Sedimentologic	Cluster C, Facies I (Upper-lower shoreface)

Cluster A: *Astarte–Cyclocardia–Glycymeris* assemblage, Cluster B: *Moerella* assemblage, Cluster C: *Glycymeris* assemblage (see Fig. 5).
[a] Corresponding bivalve assemblage and sedimentary facies are graphically shown in NMDS ordinations (see Fig. 8).

https://doi.org/10.1016/j.yqres.2013.10.015 Published online by Cambridge University Press

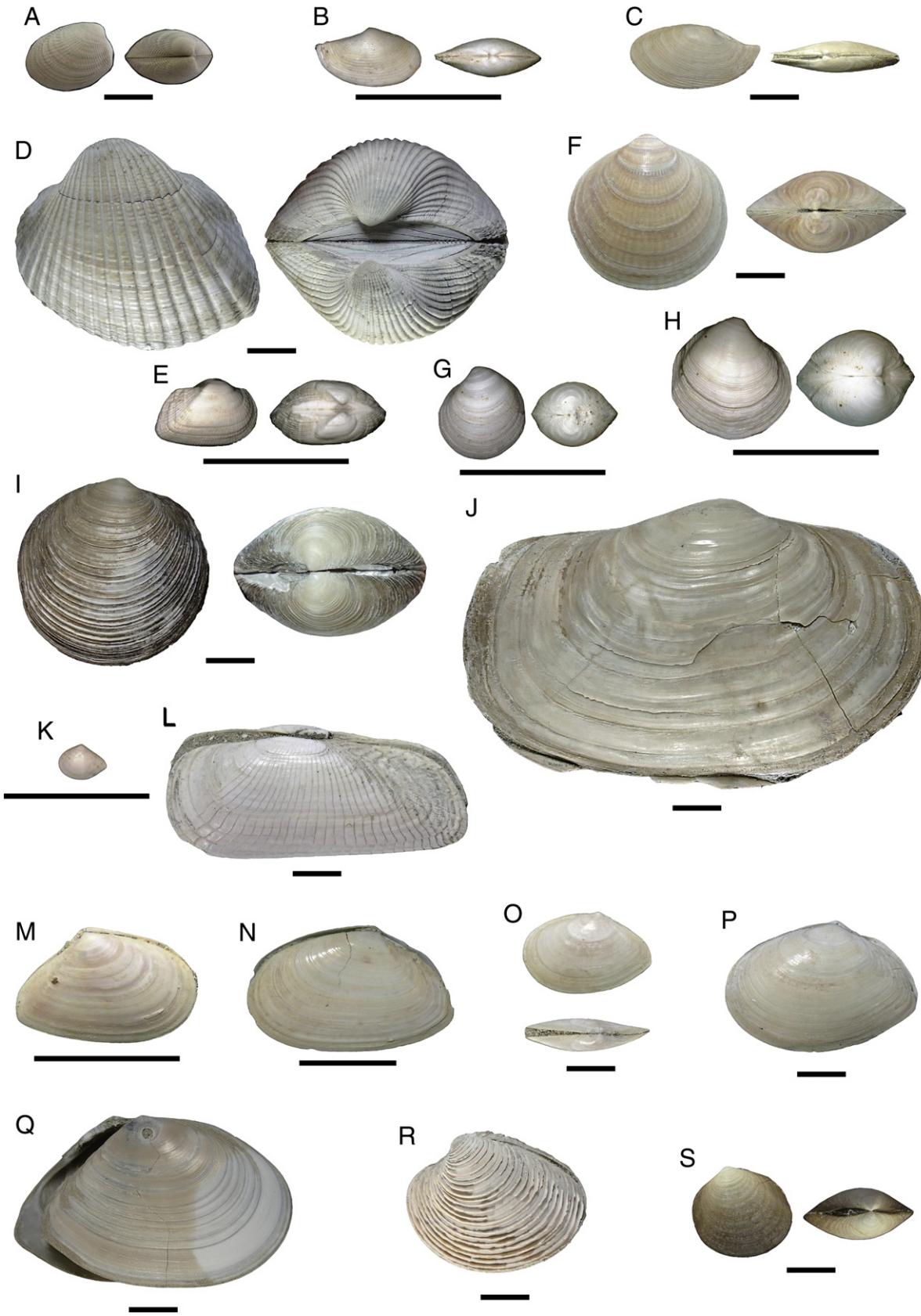

Figure 4. Autochthonous to parautochthonous bivalve fossils from both bulk and qualitative samples (A12–15 horizons). Exact sampling horizon for each specimen is shown in parentheses when it is available. A. *Acila insignis*. B. *Nuculana sematensis*. C. *Yoldia notabilis* (A12 sample). D. *Anadara* cf. *kagoshimensis*. E. *Striarca symmetrica*. F. *Glycymeris yessoensis*. G. *Pillucina pisidium*. H. *Chavania striata*. I. *Lucinoma annulatum*. J. *Panopea japonica*. K. *Leptomya cuspidariaeformis* (A13 sample). L. *Solecurtus divaricatus* (A15 sample). M. *Moerella jedoensis*. N. *Nitidotellina hokkaidoensis*. O. *Macoma praetexta*. P. *Macoma sectior*. Q. *Macoma tokyoensis*. R. *Mercenaria stimpsoni*. S. *Felaniella usta* (A13 sample). All bars = 1 cm. All specimens are deposited at the Tohoku University Museum (IGPS coll. cat. nos. 111209–111227).

https://doi.org/10.1016/j.yqres.2013.10.015 Published online by Cambridge University Press

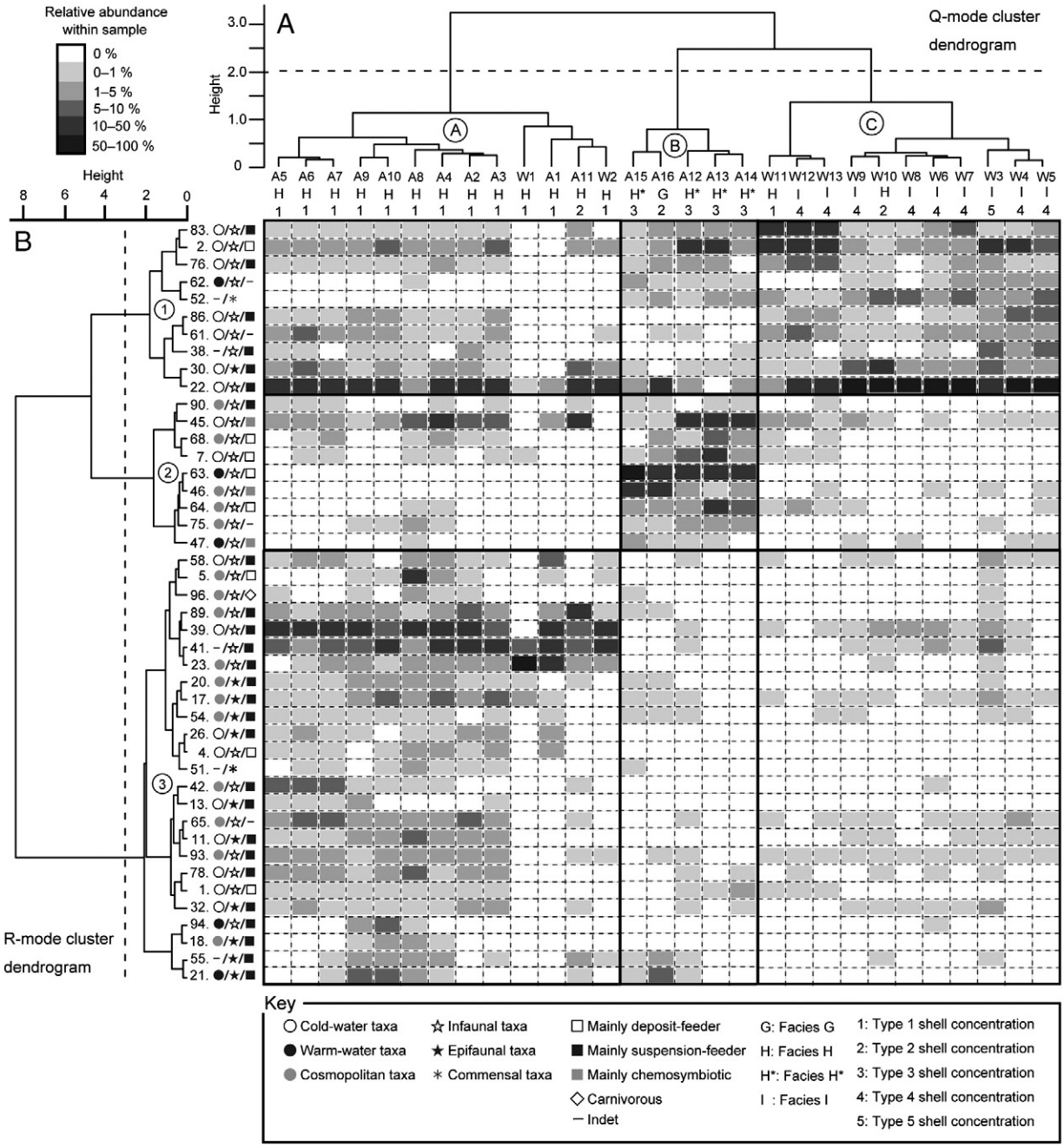

Figure 5. Cluster dendrograms and a heatmap showing matrix of relative abundance. A. Q-mode cluster dendrogram derived from Ward linkage using Bray-Curtis dissimilarity. B. R-mode cluster dendrogram derived from Ward linkage using 1-Spearman's rho. Key is shown below the heatmap. Abbreviations; 1: *Ennucula tenuis*, 2: *Acila insignis*, 4: *Nuculana pernula*, 5: *Nuculana yokoyamai*, 7: *Yoldia notabilis*, 11: *Crenella decussate*, 13: *Vilasina decorate*, 17: *Arca boucardi*, 18: *Acar plicata*, 20: *Porterius dalli*, 21: *Striarca symmetrica*, 22: *Glycymeris yessoensis*, 23: *Limopsis* spp. (*Limopsis crenata* + *Limopsis decussate* + *Limopsis* sp.), 26: *Monia macroschisma*, 30: *Mizuhopecten yessoensis*, 32: *Swiftopecten swiftii*, 38: *Limatula* spp. (*Limatula kurodai* + *Limatula vladivostokensis*), 39: *Astarte* spp. (*Astarte alaskensis* + *Astarte borealis* + *Astarte hakodatensis* + *Astarte* sp.), 41: *Cyclocardia* spp. (*Cyclocardia nipponensis* + *Cyclocardia crassidens* + *Cyclocardia* sp.), 42: *Pleuromeris pygmaea*, 45: *Axinopsida subquadrata*, 46: *Pillucina pisidium*, 47: *Chavania striata*, 51: *Kellia* sp., 52: *Nipponomysella* spp., 54: *Hiatella arctica*, 55: *Chama* sp., 58: *Ciliatocardium ciliatum*, 61: *Cadella lubrica*, 62: *Exotica miyatensis*, 63: *Moerella jedoensis*, 64: *Nitidotellina hokkaidoensis*, 65: *Macoma nipponica*, 68: *Macoma tokyoensis*, 75: *Alvenius ojianus*, 76: *Mercenaria stimpsoni*, 78: *Ezocallista brevisiphonata*, 83: *Felaniella usta*, 86: *Mactromeris polynyma*, 89: *Corbula venusta*, 90: *Penitella* sp., 93: *Myadora fluctuosa*, 94: *Myadropsis transmontana*, 96: *Plectodon ligulus*.

elements of the assemblage (cluster 3) include taxa which mainly inhabit deeper than 50 m around the Japanese Islands (e.g., *A. alaskensis*, *A. hakodatensis*, *C. nipponensis* and *Nuculana yokoyamai*; Fig. 7A), whereas taxa inhabiting shallower water in cluster 1 (e.g., *G. yessoensis* and *M. yessoensis*; Figs. 5 and 7A) are also common (Figs. 5 and 6A). Diverse epifaunal suspension-feeders in cluster 3 are characteristic of the assemblage (Fig. 5), including byssally attached (e.g., *Porterius dalli*, *Arca boucardi*, *Vilasina decorata*, *Crenella decussate*, *S. swifti*, *Acar plicata* and *Striarca symmetrica*) and cemented groups (e.g., *Monia macrochisma* and *Chama* sp.).

The *Glycymeris* assemblage (11 samples in cluster C; Fig. 5) is characterized by dominance of *G. yessoensis* (mean relative abundance ± SE = 55.1 ± 7.7; Fig. 6B). The samples of the assemblage occur in facies I of cycles 5 and 6, with exceptions of W10 (transgressive lag deposit) and W11 (intergrading horizon from facies H to I) (Figs. 2 and 5). Characteristic elements of the assemblage (cluster 1) consist of taxa which

https://doi.org/10.1016/j.yqres.2013.10.015 Published online by Cambridge University Press

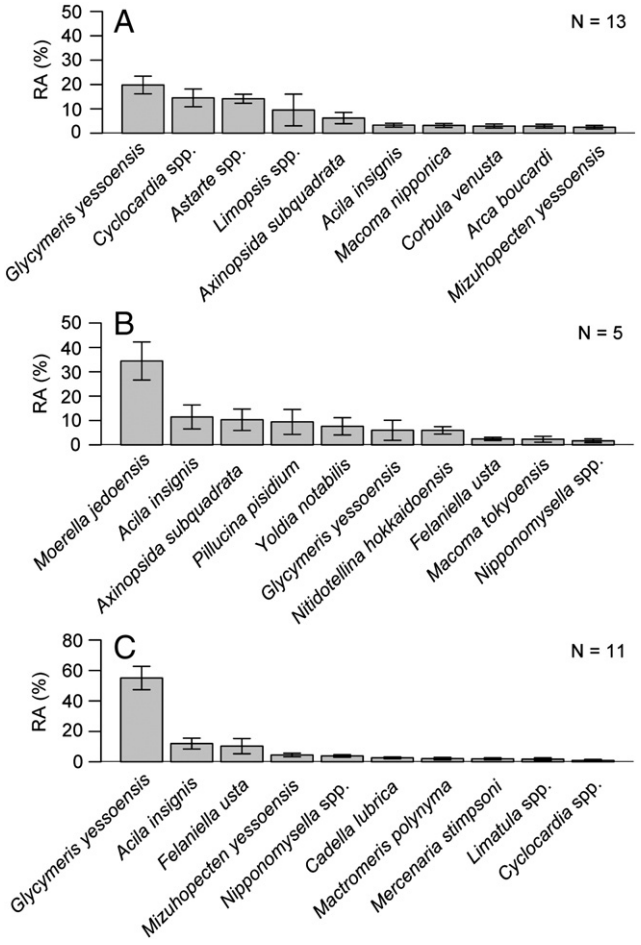

Figure 6. Composition of three bivalve assemblages. A–C. Mean relative abundance of the ten most common bivalve taxa of clusters A–C (see Fig. 5). Error bars denote standard errors. N = number of sample analyzed, RA = relative abundance.

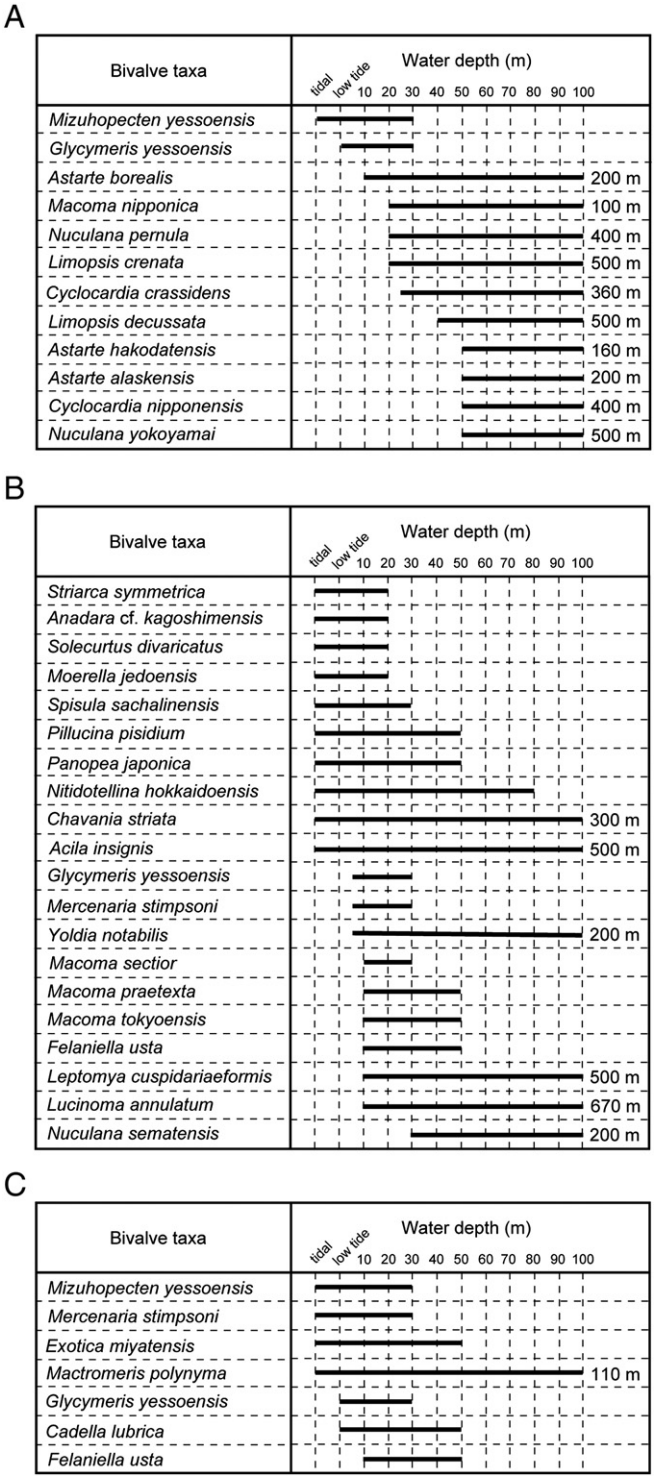

Figure 7. Bathymetric distributions of selected bivalve taxa of clusters A–C (see Fig. 5). A. Characteristic bivalve taxa of cluster A. B. Characteristic bivalve taxa of cluster B and autochthonous to parautochthonous bivalve taxa from A12–15 horizons. C. Characteristic bivalve taxa of cluster C. Data from literatures on living bivalves around the Japanese Island (Habe, 1961; Habe and Ito, 1965; Oyama, 1973; Okutani, 2000).

mainly inhabit shallower than 50 m around the Japanese Islands (e.g., *M. yessoensis*, *Mercenaria stimpsoni*, *Exotica miyatensis*, *G. yessoensis*, *Cadella lubrica* and *F. usta*; Fig. 7C). In contrast, taxa inhabiting deeper water and epifaunal groups, which are characteristic of the *Astarte–Cyclocardia–Glycymeris* assemblage, are nearly absent (Fig. 5).

The *Moerella* assemblage (5 samples in cluster B; Fig. 5) is characterized by dominance of *M. jedoensis* (mean relative abundance ± SE = 34.4 ± 7.8; Fig. 6C). The samples of the assemblage occur in facies H of cycle 6 in the Anden Coast (facies H* in Figs. 2 and 5), with an exception of A16 (regressive lag deposit). Characteristic elements of the assemblage (cluster 2) include taxa inhabiting bay (e.g., *Pillucina pisidium*, *M. tokyoensis*, *N. hokkaidoensis* and *Alveinus ojianus*) and bay to open-marine environments (e.g., *M. jedoensis* and *Yoldia notabilis*) (Fig. 5). It is noteworthy that deposit-feeding group is diverse (e.g., *M. tokyoensis*, *M. jedoensis*, *Y. notabilis* and *N. hokkaidoensis*) (Fig. 5). In addition, warm-water taxa (e.g., *M. jedoensis* and *Chavania striata*) are common in the assemblage (Fig. 5).

Ordination

The NMDS ordination reveals a separation of samples between facies G/I (shoreface) and H (inner-middle shelf), with exceptions of samples from lag deposits (W10 and A16) and intergrading horizon (W11) from facies H to I (Fig. 8A, Table 3). The significant differences in composition of the bivalve assemblages were also noted among shell-concentration types (Fig. 8B, Table 3). The assemblages defined by Q-mode cluster analysis are well separated in the ordination (Fig. 8A). The first axis segregates cluster A and the other clusters, whereas the second axis segregates cluster B and the other clusters (Fig. 8A). In addition, type 1, 3, 4/5 shell concentrations roughly correspond to clusters A–C, respectively (Fig. 8, Table 2).

https://doi.org/10.1016/j.yqres.2013.10.015 Published online by Cambridge University Press

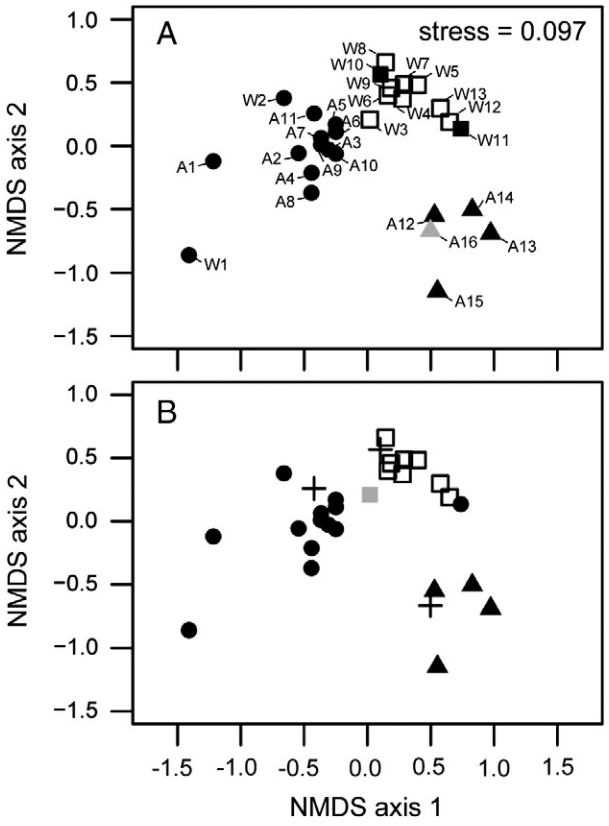

Figure 8. Two-dimensional plot of NMDS ordination. A. Samples plotted by sedimentary facies and bivalve assemblages. White, gray and black symbols denote samples from facies I, G and H, respectively. Circle, triangle and square represent cluster A–C defined by Q-mode cluster analysis (see Fig. 5). A1–16: samples from Anden Coast section, W1–13: samples from Wakimoto-2 section (see Fig. 2). B. Samples plotted by shell-concentration types. Circle, cross, triangle, white and gray squares represent type 1–5 shell concentrations, respectively. Note that type 1, 3, 4/5 shell concentrations roughly correspond to clusters A–C, respectively.

Table 3
PERMANOVA results for differences in composition of bivalve assemblages among sedimentary facies and shell-concentration types. Because multiple pairwise comparisons were applied, the Bonferroni correction was used to adjust significance level. For comparisons (d) through (f), $\alpha = 0.05/3 = 0.017$; for comparisons (g) through (l), $\alpha = 0.05/6 = 0.008$. The P-values in bold represent significant results. The P-value in italic represents insignificant result after the Bonferroni correction. SS = sum of square. MS = mean of square.

Comparison	Statistics				
	df	SS	MS	Pseudo-F	P
Global comparison					
(a) Sedimentary facies[a]	1	0.89	0.89	5.57	<**0.001**
(b) Sedimentary facies[b]	2	2.18	1.09	9.32	<**0.001**
(c) Shell-concentration type	3	2.50	0.83	7.64	<**0.001**
Pairwise comparison					
(d) Facies H vs. Facies H*[b]	1	1.29	1.29	9.81	<**0.001**
(e) Facies H vs. Facies G/I[b]	1	1.04	1.04	8.66	<**0.001**
(f) Facies H* vs. Facies G/I[b]	1	0.91	0.91	10.09	**0.001**
(g) Type 1 vs. Type 2	1	0.38	0.38	2.71	*0.021*
(h) Type 1 vs. Type 3	1	1.29	1.29	10.38	<**0.001**
(i) Type 1 vs. Type 4/5	1	1.14	1.14	10.85	<**0.001**
(j) Type 2 vs. Type 3	1	0.43	0.43	3.48	*0.033*
(k) Type 2 vs. Type 4/5	1	0.24	0.24	2.78	*0.019*
(l) Type 3 vs. Type 4/5	1	1.04	1.04	14.60	**0.002**

[a] Facies H* is not discriminated from Facies H (comparison between facies H and facies G/I).
[b] Facies H* is discriminated from Facies H (comparisons among facies H, facies H* and facies G/I).

Discussion

Bivalve assemblages and corresponding environments

Three bivalve assemblages discriminated by cluster analyses, together with corresponding shell-concentration types, indicate the following environmental and sedimentological conditions (Figs. 5 and 8, Table 2).

The *Astarte–Cyclocardia–Glycymeris* assemblage occurs in Type 1shell concentrations of facies H (Figs. 5 and 8, Table 2). The assemblage contains taxa which mainly inhabit deeper than 50 m around the Japanese Islands (Fig. 7A). This result is in agreement with analyses in sedimentary facies because facies H is formed at an inner-middle shelf (water depth = 60–100 m; Table 1). In addition, facies H intercalates layers of gravels and shells showing normal grading, bed-like geometry and sharp bases (Type 1 shell concentration; Table 2). These features suggest that the coarse-grained sediments are transported from shallower to deeper settings through storm wave/flow (Shirai and Tada, 2000). The present study supports Shirai and Tada's (2000) interpretation because the assemblage also includes thick-shelled taxa which inhabit shallower settings in poorly-preserved conditions. Specifically, we interpret that the shells were physically abraded partly because of the transportation from shallower to deeper environments (i.e., allochthonous). In addition, epifaunal taxa which attached to hard substrata are diverse in the assemblage (Fig. 5). The exotic coarse sediments transported from shallower to deeper settings probably enabled some of the epifaunal taxa to inhabit the sea floor (i.e., taphonomic feedback in Kidwell, 1986). This interpretation is reinforced by *M. modiolus* found in life orientation (i.e., autochthonous; Fig. 3B) because Stanley (1970) has confirmed that recent individuals of this species inhabit gravel bottom and byssally attached to the gravels. The diverse epifaunal suspension-feeders indicate relatively low sedimentation rate during their life span, because they have almost no ability to escape once buried (Kranz, 1974). Furthermore, higher proportion of abraded, bioeroded and encrusted shells also suggests relatively low sedimentation rate, as prolonged exposure of the shells on the sea floor over decadal period leads such taphonomic degradation of shells (e.g., Powell et al., 2011; Brett et al., 2013).

The *Glycymeris* assemblage is characterized by dominance of *G. yessoensis* and mainly occurs in Type 4/5 shell concentration of facies I (Figs. 5, 6C and 8, Table 2). The assemblage dominated by *Glycymeris* is typical for recent current-swept shoreface (Matsukuma, 1986; Thomas, 1975). These results are consistent with our analyses in sedimentary facies because facies I is interpreted as deposition at a current-swept shoreface (water depth = 5–20 m; Table 1). The inferred water depth on the basis of sedimentary facies is also supported by occurrence of *P. japonica* in life orientation (i.e., autochthonous) because this species mainly lives in the intertidal and subtidal zones (water depth < 30 m) around the Japanese Islands (Okutani, 2000). In addition, the assemblage is characterized by taxa which mainly inhabit shallower than 50 m around the Japanese Islands (Fig. 7C). Although, *G. yessoensis* shells, in Type 4 shell concentration, occur in variable states of preservation, articulated pristine shells are common. Therefore, we interpret that the *G. yessoensis* shells were reworked from the substrata but not transported outside of the shoreface habitat (i.e., parautochthonous). In general, nonsiphonate suspension-feeders, including *Glycymeris* are shallow-burrowers (Stanley, 1970; Thomas, 1975). For this reason, it is unlikely to be preserved in life orientation in high-energy settings (e.g., Kondo, 1998).

The *Moerella* assemblage is characterized by taxa inhabiting bay to open-marine conditions (Figs. 4 and 5) and thus indicative of moderately land-locked environments, such as an open bay or a bay mouth. In addition, warm-water taxa are common in the assemblage (Fig. 5), suggesting influence of the warm Tsushima Current (Fig. 1A). The late Plio-Pleistocene mollusk assemblages of the Japan Sea are characterized by appearance of warm-water taxa in sea-level highstand as a result of inflow of the warm Tsushima Current which supplies larvae of warm-

https://doi.org/10.1016/j.yqres.2013.10.015 Published online by Cambridge University Press

water organisms (e.g., Kanazawa, 1990; Kitamura et al., 1994; Nojo and Suzuki, 1999; Kitamura et al., 2000). In contrast, such a change in mollusk assemblage does not occur in the Plio-Pleistocene New Zealand cyclothem since it is deposition within a large bay sheltered from coastal currents (Beu and Kitamura, 1998). The appearance of warm-water taxa in the *Moerella* assemblage, therefore, suggests that the bay was susceptible to the warm Tsushima Current. The open bay or bay mouth, which we interpreted as environment for the *Moerella* assemblage is likely to permit the inflow of the warm Tsushima Current.

The *Moerella* assemblage mainly occurs in Type 3 shell concentration of facies H (Figs. 5 and 8, Table 2). In type 3 shell concentration, thin-shelled taxa are generally pristine and dispersed in fine-grained silty sandstone (Fig. 3D), suggesting deposition under weak influence of wave actions (open bay or bay mouth setting in the present case). Type 3 shell concentration is also characterized by occurrence of well-preserved articulated bivalves (i.e., parautochthonous; Fig. 4). In addition, some deep-borrowers are preserved in life orientation (i.e., autochthonous). We obtained the autochthonous to parautochthonous bivalves by both bulk and qualitative samplings (Fig. 4). They are used to estimate water depth by finding the water depth at which all taxa overlap on the basis of recent bathymetric distributions of the taxa around the Japanese Islands (Fig. 7B). When water depth is 20 m, most taxa (19/20) can coexist, but *Nuculana sematensis* inhabits 30–200 m, suggesting change in water depth in A12–16 horizons (Fig. 7B). In A15 sample, *S. divaricatus* (bathymetric range = 0–20 m; Figs. 4L and 7B) occurs, whereas A12 and A13–14 samples include *Y. notabilis* (bathymetric range = 5–200 m; Figs. 4C and 7B) and *F. usta* (bathymetric range = 10–50 m; Figs. 4S and 7B), respectively. For this reason, A13–14 horizons should be formed at 10–50 m in water depth. We tentatively infer 10–50 m as water depth for the *Moerella* assemblage although the difference in autochthonous to parautochthonous bivalve taxa may imply shoaling-upward trend in the horizons. More detailed reconstruction of water depth here is impossible because of wide bathymetric distributions of the bivalve taxa (Fig. 7B). Future study on sensitive bathymetric proxy (e.g., foraminifella and ostracod) may show change in water depth in the horizons.

Recognizing cryptic environmental changes

Environmental reconstruction using bivalve assemblages and their taphonomy are in agreement with that based on sedimentary facies, except for facies H of cycle 6 at the Anden Coast (facies H* in Figs. 2 and 5). Shirai and Tada (2000) have interpreted depositional environment of the horizons as an inner-middle shelf (facies H; Table 1). In contrast, the *Moerella* assemblage, which is unique to the horizons (Fig. 5), is indicative of open bay or bay mouth environment.

Our detailed observation of the sedimentary facies reveals that there are several differences between major portion (A13–15 horizons) of facies H of cycle 6 and that of the other cycles at the Anden Coast. Here, we define the former as facies H* (Table 1). Facies H intercalates distinct layers of shells and gravels (i.e., Type 1 shell concentration; Fig. 3A, Table 2), which were transported from shallower to deeper shelf by storms, while the layers are almost absent in facies H*. This difference can be explained by difference in environments. Specifically, a bay is wave-protected and thus less susceptible to storm agitation than open-marine condition. In addition, facies H* is characterized by organic fine-grained silty sandstone rich in plant fragments (Fig. 3D, Table 1). Such substrata are characteristic of highly productive waters of landlocked basins (Rhoads, 1974). Facies H*, in particular A13–14 horizons, is characterized by abundant occurrence of *Rosselia socialis* (Fig. 3D), which is a dwelling-structure of deposit-feeding terebellid polychaete (Nara, 1995). Similarly, the *Moerella* assemblage, which occurs in facies H*, contain diverse deposit-feeding bivalves (Fig. 5). The deposit-feeders achieve higher diversity and abundance on fine-grained organic substrata because it contains an abundant food supply (e.g., Rhoads and Young, 1970; Rhoads, 1974). It is, thus, probable that the organic-rich fine-grained substrata sustained the diverse deposit-feeding benthos.

On the other hand, the basal portion of cycle 6 (around A11–12 horizons) at the Anden Coast is interpreted as deposition at inner–middle shelf environment. The basal portion is associated with basal transgressive lag deposit (A11 horizon), forming a continuous widespread blanket of shells and gravels at the Anden Coast. In addition, the basal portion is characterized by distinct layers of shells and gravels (Fig. 2), which were transported from shallower to deeper settings by storms (i.e., Type 1 shell concentration; Table 2). These observations suggest that the basal portion was deposition at almost open-marine condition because the characteristic sediments should be formed at wave-dominated environment. Although the bivalve assemblage from A12 horizon is categorized as a *Moerella* assemblage, it contains small number of *Astarte* spp. and *Cyclocardia* spp., which are characteristic taxa of inner–middle shelf environment (i.e., the *Astarte–Cyclocardia–Glycymeris* assemblage; Figs. 5 and 7A). This result indicates that A12 horizon is environmentally condensed because of low sedimentation rate and intense bioturbation. This inference is supported by characteristic architecture of the sedimentary cycle. Specifically, cycle 6 at the Anden Coast consists of thinner deepening-upward succession and thicker shoaling-upward succession (Fig. 2), suggesting asymmetric pattern of glacio-eustatic sea-level changes with rapid transgression and/or low sediment supply into the sea during transgression (Shirai and Tada, 2000). Consequently, facies H of cycle 6 at the Anden Coast in Shirai and Tada (2000) is subdivided into the lower facies H (around A11–12 horizons) and the upper facies H* (A13–16 horizons), and their boundary is gradual because of low sedimentation rate and intense bioturbation (Fig. 2).

Our analyses in bivalve assemblages also refine interpretation of depositional dynamics. The lower part of cycle 6 at the Anden Coast consists of facies C, G*, H and H*, and they were deposited under minor influence of wave actions despite the nearshore settings, with an exception of facies H (Fig. 2, Table 1). In addition, facies C is underlain by facies B, which represents a flood plain and a river channel (Fig. 2, Table 1). Facies B, C and G* are interpreted as combination of typical facies for estuarine systems (e.g., Dalrymple et al., 1992; Allen and Posamentier, 1993) (Fig. 9A, B). The depositional environment changed to an inner–middle shelf (facies H) and then a bay mouth to an open bay (facies H*) associated with sea-level fluctuation (Fig. 9C) during MIS 6.0–5.4 because of chronostratigraphic position of the Toya tephra (MIS 5.5–5.4; Machida and Arai, 2003) and basal transgressive lag (MIS 6.2–6.0; Shirai and Tada, 2000). Facies H* is overlain by relatively organic-poor sediments with various sedimentary structures (facies E, F and G; Fig. 2; Table 1), suggesting change in wave conditions. The bay might be rapidly filled seaward with prograding sediment owing to large amount of sediment from rivers because the characteristic carbonaceous facies (facies C, G* and H*; Fig. 3D, Table 1) imply importance of river discharge as the sediment supply. Furthermore, land-locked basins, including an estuary and a bay is highly efficient sediment trap. It is, therefore, possible that depositional environment changed from bay to open marine conditions because the bay was filled with the sediment after deposition of facies H*.

This study clearly shows that combination of analyses in sedimentary facies and fossil assemblages leads to better understandings of environments and depositional dynamics. As Shirai and Tada (2000) have not distinguished the facies H and H*, minor differences in these facies may be difficult to detect. It has been shown that fossil assemblages can be more sensitive to environmental changes than sedimentary facies, in particular intensely bioturbated silty facies (e.g., Brett, 1995, 1998; Holland et al., 2001) and massive sandy facies (e.g., Daley, 2002). However, strata without fossils are impossible to analyze fossil assemblages, and thus sedimentary facies are of utmost importance for reconstructing environment. Although, we collected bivalve fossils from four sedimentary facies (facies G, H, H* and I; Fig. 2), the other facies did not contain shells with reasonable sample sizes for statistical analyses, and thus the environmental interpretation largely depends

https://doi.org/10.1016/j.yqres.2013.10.015 Published online by Cambridge University Press

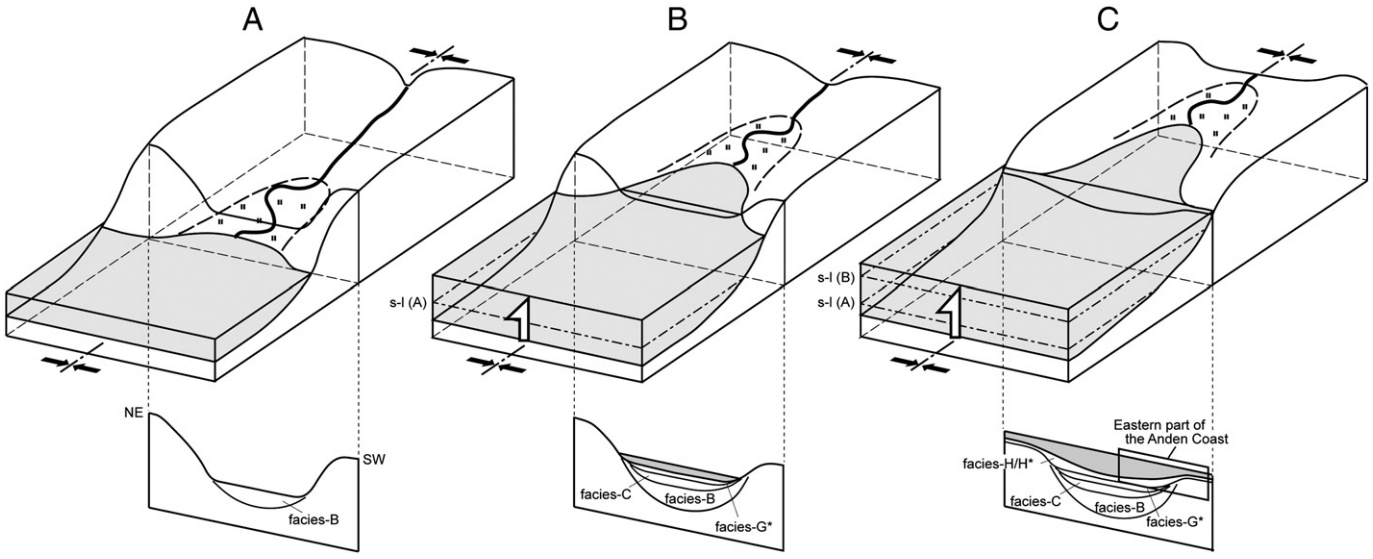

Figure 9. Schematic illustration of geological evolution at the Anden Coast during formation of the lower part of cycle 6 (MIS 6.2–5.4). Note that cycle 6 at the Anden Coast is deposition between the tilting hinge and syncline axis, which are formed by local crustal movement. A. Lowstand. Flood plain and river channel (facies B). B. Lowstand to initiation of transgression. An incised valley was drowned and became an estuary. Organic-rich facies (facies C and G*) were interpreted as characteristic components of the estuarine system. C. Transgression to maximum marine flooding. Transgressive surface eroded the underlying strata. The depositional environment changed from inner-middle shelf (facies H) to bay mouth or open bay environments (facies H*), accompanying with slight sea-level fall.

on analyses in sedimentary facies. Fortunately, environmental reconstruction on the basis of sedimentary facies and fossil assemblages is reciprocal. Specifically, primary sedimentary structures are expected to be preserved in the cases where organisms are scarce, whereas the sedimentary structures can be destroyed owing to intense bioturbation if organisms are abundant. In the massive facies, fossils are likely to be preserved, and thus multivariate analyses of fossil assemblages can be used as in this study. We emphasize that fossil assemblages can be powerful tool to reconstruct environment even in monotonous sedimentary facies, which may be difficult to detect environmental changes by analyses in sedimentary facies alone.

Causes of environmental changes

Both in cluster analyses and NMDS ordination, samples from lag deposits (W10 and A16) and intergrading horizon from facies H to I (W11) clustered with samples from other sedimentary facies (Figs. 5 and 8A). It is not surprising because lag deposits are accumulated by reworking underling strata. For W1 sample, the score of the first axis is the lowest, showing anomalous position in the NMDS ordination (Fig. 8A). In W1 sample, *Limopsis* spp. explains 85.5% of the bivalve assemblage (Fig. 5). Recent *Limopsis* often shows patchy distribution (e.g., Ito, 1989; Kondo, 1989), and thus W1 sample probably reflected an aggregation of *Limopsis* spp. by chance. The patchy distribution can be preserved in fossil assemblages and affect composition of fossil assemblages (e.g., Holland, 2005).

The NMDS ordination shows assemblages along two environmental gradients, a bathymetrical one and the other related to open-marine and bay conditions (Fig. 8). In the NMDS ordination (Fig. 8), the first axis segregates cluster A and the other clusters. We estimated water depths of clusters A–C as 50 m < 10-50 m and <30 m, respectively. Therefore, the first axis may represent water depth and the score tends to be high with decreasing water depth. The second axis segregates cluster B and the other clusters. We interpret environment of cluster B as an open bay or a bay mouth. For this reason, the second axis is related to bay and open-marine conditions, and the score tends to be lower in bay condition and vice-versa for open-marine condition.

Bivalve assemblages represented by clusters A and C contain samples from different sedimentary cycles and localities, suggesting repetitive changes in environment (Figs. 5 and 8A). In addition, clusters A (water depth > 50 m) and C (water depth < 30 m) mainly correspond to facies H (water depth = 60–100 m) and I (water depth = 5–20 m), respectively (Figs. 5 and 8A, Table 2). These results suggest that the paleoecological patterns reflect sea-level changes. It is not surprising because Shirai and Tada (2000) have showed that the sedimentary cycles at the Anden Coast faithfully reflect fifth- and sixth-order glacio-eustatic sea-level changes.

The *Moerella* assemblage (cluster B), which represents moderately land-locked environments, is unique to facies H* of cycle 6 at the Anden Coast (Figs. 5 and 8A, Table 2). Specifically, the *Glycymeris* assemblage (cluster C), which is indicative of open-marine environment, occurs in probable cycle 6 of Wakimoto-2 section (W10–13; Figs. 5 and 8A). These results imply that the environmental change from open-marine to land-locked conditions at the Anden Coast cannot be explained by glacio-eustatic sea-level changes alone. In addition to the sea-level changes, local crustal movement probably triggered the environmental changes. Multiple reverse faults and folds trending N–S to NNW–SSE affect the Quaternary formations around the Anden Coast (Fig. 1C). At the Anden Coast, the dip angle decreases upward from 54° to 5°, suggesting that crustal tilting continued concurrently with sedimentation (Shirai and Tada, 2002). In addition, Shirai and Tada (2002) have showed that subsidence around the Anden Coast was caused mainly by the crustal tilting with a fixed tilting hinge associated with folding after ca. 450 ka. The eastern part of the Anden Coast is located between the tilting hinge (Shirai and Tada, 2002) and syncline axis which has been estimated from distribution of the Shibikawa and Wakimoto formations (Kano et al., 2011). The Anden Coast, therefore, was a moderately land-locked basin during deposition of facies H* (Fig. 9). We conclude that the local crustal subsidence affected coastal geomorphology around the Anden Coast and formed the land-locked basin at the time of facies H* deposition. This study suggests that local crustal movement affects coastal geomorphology and thus is also an important factor to cause changes in sedimentary dynamics and fossil assemblages in tectonically active basins.

Conclusions

We reconstructed environments using paleoecology and taphonomy of bivalve assemblages from the Pleistocene of Oga Peninsula, northern Japan, with particular attention paid to relationship between the

https://doi.org/10.1016/j.yqres.2013.10.015 Published online by Cambridge University Press

bivalve assemblages and sedimentary facies. Three assemblages are recognized by cluster analyses. The *Astarte–Cyclocardia–Glycymeris* assemblage is indicative of shelf environment (below the storm wave base) where gravels and shells are transported from shallower settings. Supply of the exotic coarse sediment probably enabled epifaunal taxa to inhabit the sea floor. The assemblage, therefore, is mixture of ecologically unrelated taxa. The *Glycymeris* assemblage is characterized by dominance of *G. yessoensis* and represents current-swept shoreface environment (above the storm wave base). *Glycymeris yessoensis* is interpreted as parautochthonous. The *Moerella* assemblage is characterized by taxa inhabiting bay to open-marine conditions and diverse deposit-feeders, indicating moderately land-locked environments, such as an open bay or a bay mouth. Most of the taxa in the assemblage are interpreted as parautochthonous. Fine-grained substrata rich in organic matters in the bay were probably suitable for deposit-feeding benthos (bivalves and polychaetes in the present case). This study suggests that glacio-eustatic sea-level changes and local crustal movement are important factors to cause changes in fossil assemblages and sedimentary dynamics.

This study suggests that fossil assemblages can be a powerful tool to reconstruct environment even in massive sedimentary facies (shelf and bay in the present case), which may be difficult to reconstruct environment, based solely on sedimentary facies. Overall, we clearly show that combination of analyses in sedimentary facies and fossil assemblages leads to better understandings of environments and depositional dynamics.

Supplementary data to this article can be found online at http://dx.doi.org/10.1016/j.yqres.2013.10.015.

Acknowledgments

The authors thank A. Gillespie (University of Washington), M. Zuschin (University of Vienna) and A. Tomašových (Slovak Academy of Sciences) for helpful comments on the manuscript, A. Watanabe (Polder Museum of Ogata-Mura) for providing information on stratigraphy, N. Kotake (Chiba University) and H. Kato (Tohoku University) for discussion and encouragement, A. Matsukuma (The Kyushu University Museum) and H. Fukuda (Okayama University) for advice on identification of bivalve fossils, K. Kanazawa (Kanagawa University) for identification of echinoid fossils, G. Kanaya (National Institute for Environmental Studies) for providing literatures on feeding ecology of benthos, H. Torii for help in collecting bulk samples at the Anden Coast, J. Nemoto (Tohoku University) for registration of our macrofossil specimens and H. Kano (The Tohoku University Museum) for instruction in microscope use. Sample collections at the Anden Coast were performed with permission of Akita Prefecture.

References

Abbott, S.T., 1997. Mid-cycle condensed shellbeds from mid-Pleistocene cyclothems, New Zealand: implications for sequence architecture. Sedimentology 44, 805–824.
Abbott, S.T., Carter, R.M., 1997. Macrofossil associations from Mid-Pleistocene cyclothems, Castlecliff section, New Zealand: implications for sequence stratigraphy. Palaios 12, 188–210.
Allen, G.P., Posamentier, H.W., 1993. Sequence stratigraphy and facies model of an incised valley fill: the Gironde estuary, France. Journal of Sedimentary Petrology 63, 378–391.
Anderson, M.J., 2001. A new method for non-parametric multivariate analysis of variance. Austral Ecology 26, 32–46.
Beu, A., Kitamura, A., 1998. Exposed coasts vs sheltered bays: contrast between New Zealand and Japan in the molluscan record of temperature change in Plio-Pleistocene cyclothems. Sedimentary Geology 122, 129–149.
Borcard, D., Gillet, F., Legendre, P., 2011. Numerical Ecology with R. Springer.
Brett, C.E., 1995. Sequence stratigraphy, biostratigraphy, and taphonomy in shallow marine environments. Palaios 10, 597–616.
Brett, C.E., 1998. Sequence stratigraphy, paleoecology, and evolution: biotic clues and responses to sea-level fluctuations. Palaios 13, 241–262.
Brett, C.E., Parsons-Hubbard, K.M., Walker, S.E., Ferguson, C., Powell, E.N., Staff, G., Ashton-Alcox, K.A., Raymond, A., 2013. Gradients and patterns of sclerobionts on experimentally deployed bivalve shells: synopsis of bathymetric and temporal trends on a decadal time scale. Palaeogeography, Palaeoclimatology, Palaeoecology 312, 278–304.
Bush, A.M., Brame, R.I., 2010. Multiple paleoecological controls on the composition of marine fossil assemblages from the Frasnian (Late Devonian) of Virginia, with a comparison of ordination methods. Paleobiology 36, 573–591.
Carboni, M.G., Bergamin, L., Bella, L.D., Esu, D., Cerone, E.P., Antonioli, F., Verrubbi, V., 2010. Palaeoenvironmental reconstruction of late Quaternary foraminifera and molluscs from the ENEA borehole (Versilian plain, Tuscany, Italy). Quaternary Research 74, 265–276.
Clarke, K.R., 1993. Non-parametric multivariate analyses of changes in community structure. Australian Journal of Ecology 18, 117–143.
Daley, G.M., 2002. Creating a paleoecological framework for evolutionary and paleoecological studies: an example from the Fort Thompson Formation (Pleistocene) of Florida. Palaios 17, 419–434.
Daley, G.M., Ostrowski, S., Geary, D.H., 2007. Paleoenvironmentally correlated differences in a classic predator–prey system: the bivalve *Chione elevate* and its gastropod predators. Palaios 22, 166–173.
Dalrymple, R.W., Zaitlin, B.A., Boyd, R., 1992. Estuarine facies models: conceptual basis and stratigraphic implications. Journal of Sedimentary Petrology 62, 1130–1146.
Dominici, S., 2001. Taphonomy and paleoecology of shallow marine macrofossil assemblages in a collisional setting (Late Pliocene–Early Pleistocene, Western Emilia, Italy). Palaios 16, 336–353.
Dominici, S., Conti, C., Benvenuti, M., 2008. Foraminifer communities and environmental change in marginal marine sequences (Pliocene, Tuscany, Italy). Lethaia 41, 447–460.
Greenwood, B., Davidson-Arnott, R.G.D., 1979. Sedimentation and equilibrium in wave-formed bars: a review and case study. Canadian Journal of Earth Sciences 16, 312–332.
Habe, T., 1961. Colored Illustrations of the Shells of Japan, volume 2. Hoikusha Publishing, Osaka (in Japanese).
Habe, T., Ito, K., 1965. Shells of the World in Color, Volume 1: The Northern Pacific. Hoikusha Publishing, Osaka (in Japanese).
Hendy, A.J.W., Kamp, P.J.J., 2004. Late Miocene–Early Pliocene biofacies of Wanganui and Taranaki Basins, New Zealand: applications to paleoenvironmental and sequence stratigraphic analysis. New Zealand Journal of Geology and Geophysics 47, 769–785.
Hendy, A.J.W., Kamp, P.J.J., 2007. Paleoecology of Late Miocene–Early Pliocene sixth-order glacioeustatic sequences in the Manutahi-1 core, Wanganui-Taranaki Basin, New Zealand. Palaios 22, 325–337.
Holland, S.M., 2005. The signatures of patches and gradients in ecological ordinations. Palaios 20, 573–580.
Holland, S.M., Miller, A.I., Meyer, D.L., Dattilo, B.F., 2001. The detection and importance of subtle biofacies within a single lithofacies: the Upper Ordovician Kope Formation of the Cincinnati, Ohio, region. Palaios 16, 205–217.
Horikoshi, M., 1962. Warm temperate region and coastal-water area in the marine biogeography of the shallow sea system around the Japanese islands. The Quaternary Research 2, 117–124 (in Japanese with English abstract).
Huber, M., 2010. Compendium of Bivalves. ConchBooks, Hackenheim.
Huzioka, K., Takayasu, T., Matoba, Y., 1970. The Kamayachi Formation (Pleistocene), Oga Peninsula, Northeast Japan. Journal of the Mining College, Akita University, Series A 4, 35–50.
Imbrie, J., Hays, J.D., Martinson, D.G., McIntyre, A., Mix, A.C., Morlay, J.J., Pisias, N.G., Prell, W.L., Shackleton, N.J., 1984. The orbital theory of Pleistocene climates: support from a revised chronology of the marine $\delta^{18}O$ record. In: Berger, A., Imbrie, J., Hays, G., Kukla, G., Saltzman, B. (Eds.), Milankovitch and Climate, Part 1. Plenum Reidel, Dordrecht, pp. 269–305.
Ito, K., 1989. Distribution of molluscan shells in the coastal areas of Chuetsu, Kaetsu and Sado Island, Niigata Prefecture, Japan. Bulletin of the Japan Sea Regional Fisheries Research Laboratory 39, 37–133 (in Japanese with English abstract).
Ito, M., Nishikawa, T., Sugimoto, H., 1999. Tectonic control of high-frequency depositional sequences with durations shorter than Milankovitch cyclicity: an example from the Pleistocene paleo-Tokyo Bay, Japan. Geology 27, 763–766.
Japanese Association of Benthology, 2012. Threatened Animals of Japanese Tidal Flats: Red Data Book of Seashore Benthos. Tokai University Press, Tokyo (in Japanese).
Kanazawa, K., 1990. Early Pleistocene glacio-eustatic sea-level fluctuations as deduced from periodic changes in cold- and warm-water molluscan associations in the Shimokita Peninsula, Northeast Japan. Palaeogeography, Palaeoclimatology, Palaeoecology 79, 263–273.
Kano, K., Ohguchi, T., Yanagisawa, Y., Awata, Y., Kobayashi, N., Sato, Y., Hayashi, S., Kitazato, H., Ogasawara, K., Komazawa, M., 2011. Geology of the Toga and Funakawa District, Quadrangle Series, 1:50,000. Geological Survey of Japan, AIST, Tsukuba (in Japanese with English abstract).
Kato, M., Watanabe, A., 1976. On geologic structure and the depositional condition of the Pleistocene deposits at the Anden coast, Oga Peninsula, Northeast Japan. Annual Report of Akita Prefectural Museum 1, 56–65 (in Japanese with English abstract).
Kidwell, S.M., 1986. Taphonomic feedback in Miocene assemblages: testing the role of dead hardparts in benthic communities. Palaios 1, 239–255.
Kidwell, S.M., 1991. The stratigraphy of shell concentrations. In: Allison, P.A., Briggs, E.G. (Eds.), Taphonomy: Releasing the Data Locked in the Fossil Record, Volume 9 of Topics in Geobiology. Plenum Press, New York, pp. 211–290.
Kidwell, S.M., Holland, S.M., 1991. Field description of coarse bioclastic fabrics. Palaios 6, 426–434.
Kidwell, S.M., Fürsich, F.T., Aigner, T., 1986. Conceptual framework for the analysis and classification of fossil concentrations. Palaios 1, 228–238.
Kitamura, A., Kondo, Y., Sakai, H., Horii, M., 1994. Cyclic changes in lithofacies and molluscan content in the early Pleistocene Omma Formation, Central Japan related to the 41,000-year orbital obliquity. Palaeogeography, Palaeoclimatology, Palaeoecology 112, 345–361.
Kitamura, A., Omote, H., Oda, M., 2000. Molluscan response to early Pleistocene rapid warming in the Sea of Japan. Geology 28, 723–726.

Kitazato, H., 1975. Geology and geochronology of the younger Cenozoic of the Oga Peninsula. Contributions from the Institute of Geology and Paleontology, Tohoku University, 75, pp. 17–49 (in Japanese with English abstract).
Kondo, Y., 1989. 'In situ' observation of a bathyal bivalve *Limopsis tajimae* by means of box core sampling, with comparative description of the fossil counterparts. Venus 48, 27–39.
Kondo, Y., 1998. Adaptive strategies of suspension-feeding, soft-bottom infaunal bivalves to physical disturbance: evidence from fossil preservation. In: Paul, A.J., Haggart, J.W. (Eds.), Bivalves: An Eon of Evolution — Paleobiological Studies Honoring Norman D. University of Calgary Press, Newell, pp. 377–391.
Kondo, Y., Abbott, S.T., Kitamura, A., Kamp, P.J.J., Naish, T.R., Kamataki, T., Saul, G.S., 1998. The relationship between shellbed type and sequence architecture: examples from Japan and New Zealand. Sedimentary Geology 122, 109–127.
Kranz, P.M., 1974. The anastrophic burial of bivalves and its paleoecological significance. Journal of Geology 82, 237–265.
Kurihara, T., Takami, H., Kosuge, T., Chiba, S., Iseda, M., Sasaki, T., 2011. Area-specific temporal changes of species composition and species-specific range shifts in rocky-shore mollusks associated with warming Kuroshio Current. Marine Biology 158, 2095–2107.
Legendre, P., Gallagher, E.D., 2001. Ecologically meaningful transformations for ordination of species data. Oecologia 129, 271–280.
Legendre, P., Legendre, L., 2012. Numerical Ecology, Third English edition. Elsevier Science.
Leonard-Pingel, J.S., Jackson, J.B.C., O'Dea, A., 2012. Changes in bivalve functional and assemblage ecology in response to environmental change in the Caribbean Neogene. Paleobiology 38, 509–524.
Machida, H., Arai, F., 2003. Atlas of Tephra In and Around Japan, New Edition. University of Tokyo Press (in Japanese).
Matsukuma, A., 1986. Cenozoic Glycymeridid bivalves of Japan. Palaeontological Society of Japan Special Papers 29, 78–94.
Minchin, P.R., 1987. An evaluation of the relative robustness of techniques for ecological ordination. Vegetatio 69, 89–107.
Nara, M., 1995. *Rosselia socialis*: a dwelling structure of a probable terebellid polychaete. Lethaia 28, 171–178.
Nojo, A., Suzuki, A., 1999. Taphonomy of shell concentrations: reconstruction of depositional processes by combined analyses of mollusc and foraminifer. Memories of Geological Society of Japan 54, 35–54 (in Japanese with English abstract).
Ogasawara, K., Masuda, K., Matoba, Y., 1986. Neogene and Quaternary Molluscs from the Akita Oil-field, Japan. Commemorative Association of Professor Taisuke Takayasu's Retirement and Supporters' Fundation of Mineral Industry Museum. Mining College, Akita University (in Japanese).
Okada, Y., 1979. Stratigraphy and ostracoda from late Cenozoic strata of the Oga Peninsula, Akita Prefecture. Transactions and Proceedings of the Palaeontological Society of Japan, New Series 115, 143–173.
Oksanen, J., Blanchet, F.G., Kindt, R., Legendre, P., Minchin, P.R., O'Hara, R.B., Simpson, G.L., Solymos, P., Stevens, M.H.H., Wagner, H., 2012. Vegan: Community Ecology Package. <http://cran.r-project.org/web/packages/vegan/index.html> Accessed on 30 December 2012.
Okutani, T., 2000. Marine Mollusks in Japan. Tokai University Press, Tokyo (in Japanese with English captions).
Oyama, K., 1973. Revision of Matajiro Yokoyama's type mollusca from the Tertiary and Quaternary of the Kanto area. Palaeontological Society of Japan Special Papers 17, 1–148.
Powell, E.N., Staff, G.M., Callender, W.R., Ashton-Alcox, K.A., Brett, C.E., Parsons-Hubbard, K.M., Walker, S.E., Raymond, A., 2011. Taphonomic degradation of molluscan remains during thirteen years on the continental shelf and slope of the northwestern Gulf of Mexico. Palaeogeography, Palaeoclimatology, Palaeoecology 312, 209–232.
R Development Core Team, 2009. R: A Language and Environment for Statistical Computing. R Foundation for Statistical Computing, Vienna, Austria3-900051-07-0 (http://www.R-project.org. Accessed on 17 February 2012).
Reimnitz, E., Toimil, L.J., Shepard, F.P., Gutiérrez-Estrada, M., 1976. Possible rip current origin for bottom ripple zones, to 30-m depth. Geology 4, 395–400.
Rhoads, D.C., 1974. Organism-sediment relations on the muddy sea floor. Oceanography and Marine Biology: An Annual Review 12, 263–300.
Rhoads, D.C., Young, D.K., 1970. The influence of deposit-feeding organisms on sediment stability and community trophic structure. Journal of Marine Research 28, 150–178.
Rhoads, D.C., Speden, I.G., Waage, K.M., 1972. Trophic group analysis of Upper Cretaceous (Maestrichtian) bivalve assemblages from South Dakota. The American Association of Petroleum Geologists Bulletin 56, 1100–1113.
Saito, Y., 1988. Relation between coastal topography, sediments, and depth of wave base. Earth Monthly 10, 458–466 (in Japanese).
Saito, Y., 1989. Classification of shelf sediments and their sedimentary facies in the storm-dominated shelf: a review. Journal of Geography 98, 164–179 (in Japanese with English abstract).
Scarponi, D., Kowalewski, M., 2004. Stratigraphic paleoecology: bathymetric signatures and sequence overprint of mollusk associations from upper Quaternary sequences of the Po Plain, Italy. Geology 32, 989–992.
Shirai, M., Tada, R., 1997. Cyclostratigraphy of the upper Quaternary shallow-marine sediments at the Anden Coast, Oga Peninsula. Journal of the Sedimentological Society of Japan 44, 43–52 (in Japanese with English abstract).
Shirai, M., Tada, R., 2000. Sedimentary successions formed by fifth-order glacio-eustatic cycles in the middle to upper Quaternary formations of the Oga Peninsula, Northeast Japan. Journal of Sedimentary Research 70, 839–849.
Shirai, M., Tada, R., 2002. High-resolution reconstruction of Quaternary crustal movement based on sedimentary facies analysis: an example from the Oga Peninsula, Northern Japan. Journal of Sedimentary Research 72, 386–392.
Shirai, M., Tada, R., Fujioka, K., 1997. Identification and chronostratigraphy of middle to upper Quaternary marker tephras occurring in the Anden Coast based on comparison with ODP cores in the Sea of Japan. The Quaternary Research 36, 183–196 (in Japanese with English abstract).
Shiraishi, T., 2000. The Iriai Formation: a newly defined marine terrace deposit correlative with oxygen isotope stage 5a in the Oga Peninsula, Akita Prefecture, Northeast Japan. Daishiki 32, 1–10 (in Japanese).
Shiraishi, T., Arai, F., Fujimoto, Y., 1992. Discovery of Aso-4 ash and drift pumice of Aso-4 pyroclastic flow and Sambe-Kisuki pumice fall deposits in the Upper Quaternary of the Oga Peninsula, Akita Prefecture, Northeast Honshu, Japan. The Quaternary Research 31, 21–27 (in Japanese with English abstract).
Shiraishi, T., Shirai, M., Nishikawa, O., Suzuki, H., Furuhashi, K., Hoshi, T., 2008. Geomorphology and Quaternary geology of the Oga-Noshiro area, Akita Prefecture. The Journal of the Geological Society of Japan 114, 33–50 (Supplement, in Japanese).
Shuto, T., Takayasu, T., Iwai, T., Kamada, Y., Nishioka, K., Otsuka, T., Kotaka, T., Masuda, K., Ogasawara, K., Noda, K., Chinzei, K., Kanie, Y., Okamoto, K., Matsukuma, A., Iwasaki, Y., 1977. Stratigraphic relation of the Shibikawa, Anden and Katanishi formations in the Oga Peninsula, North Honshu, Japan. Science Reports, 12. Department of Geology, Kyushu University, pp. 215–227 (in Japanese with English abstract).
Stanley, S.M., 1970. Relation of shell form to life habits of the bivalvia (Mollusca). The Geological Society of America, Inc. Memoir 125, 1–296.
Takayasu, T., 1962. Molluscan fossils from the Shibikawa Formation in the Oga Peninsula, Akita prefecture, Japan—studies of the Cenozoic fauna in the Akita oil field, part 2. Journal of the Mining College, Akita University, Series A 2, 1–19.
Thomas, R.D.K., 1975. Functional morphology, ecology, and evolutionary conservatism in the Glycymerididae (Bivalvia). Palaeontology 18, 217–254.
Todd, J.A., Jackson, J.B.C., Johnson, K.G., Fortunato, H.M., Heitz, A., Alvarez, M., Jung, P., 2002. The ecology of extinction: molluscan feeding and faunal turnover in the Caribbean Neogene. Proceedings of the Royal Society of London B 296, 571–577.
Tomašových, A., Zuschin, M., 2009. Variation in brachiopod preservation along a carbonate shelf-basin transect (Red Sea and Gulf of Aden): environmental sensitivity of taphofacies. Palaios 24, 697–716.
Wada, K., Nishihira, M., Furota, T., Nojima, S., Yamanishi, R., Nishikawa, T., Goshima, S., Suzuki, T., Kato, M., Shimamura, K., Fukuda, H., 1996. Present status of estuarine locales and benthic invertebrates occurring in estuarine environments in Japan. WWF Japan Science Report 3, 1–182 (in Japanese).
Watanabe, A., 2004. Molluscan fossils from the Pleistocene Iriai Formation in the Oga Peninsula, Akita Prefecture, Japan. Akita Chigaku 55, 1–10 (in Japanese).
Zecchin, M., 2005. Relationships between fault-controlled subsidence and preservation of shallow-marine small-scale cycles: example from the lower Pliocene of the Crotone Basin (Southern Italy). Journal of Sedimentary Research 75, 300–312.
Zuschin, M., Harzhauser, M., Mandic, O., 2007. The stratigraphic and sedimentologic framework of fine-scale faunal replacements in the Middle Miocene of the Vienna Basin (Austria). Palaios 22, 285–295.

https://doi.org/10.1016/j.yqres.2013.10.015 Published online by Cambridge University Press